Identification of Neuropeptide S Antagonists: Structure–Activity Relationship Studies, X-ray Crystallography, and in Vivo Evaluation

Carla Hassler,[†] Yanan Zhang,[†] Brian Gilmour,[†] Tyler Graf,[†] Timothy Fennell,[†] Rodney Snyder,[†] Jeffrey R. Deschamps,[§] Rainer K. Reinscheid,[‡] Celia Garau,[‡] and Scott P. Runyon*[,†]

[†]Research Triangle Institute, Post Office Box 12194, Research Triangle Park, North Carolina 27709-2194, United States
[‡]Department of Pharmaceutical Sciences, University of California, Irvine, 2214 Natural Sciences I, Mail Code: 3958, Irvine, California 92697-3958, United States
[§]Center for Bio/Molecular Science and Engineering, Naval Research Laboratory, Code 6930, 4555 Overlook Avenue SW, Washington, DC 20375, United States

Ⓢ *Supporting Information*

ABSTRACT: Modulation of the neuropeptide S (NPS) system has been linked to a variety of CNS disorders such as panic disorder, anxiety, sleeping disorders, asthma, obesity, PTSD, and substance abuse. In this study, a series of diphenyltetrahydro-1H-oxazolo[3,4-α]pyrazin-3(5H)-ones were synthesized and evaluated for antagonist activity at the neuropeptide S receptor. The absolute configuration was determined by chiral resolution of the key synthetic intermediate, followed by analysis of one of the individual enantiomers by X-ray crystallography. The R isomer was then converted to a biologically active compound (**34**) that had a K_e of 36 nM. The most potent compound displayed enhanced aqueous solubility compared with the prototypical antagonist SHA-68 and demonstrated favorable pharmacokinetic properties for behavioral assessment. In vivo analysis in mice indicated a significant blockade of NPS induced locomotor activity at an ip dose of 50 mg/kg. This suggests that analogs having improved drug-like properties will facilitate more detailed studies of the neuropeptide S receptor system.

KEYWORDS: Neuropeptide S, structure–activity relationship, NPSR
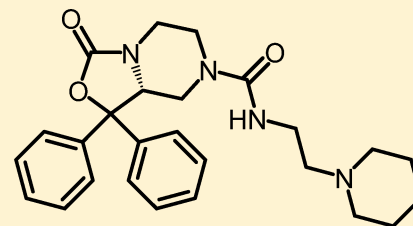
Compound 34; NPSR 107I Ke = 36 nM

The discovery and evaluation of numerous neuropeptides is beginning to broaden our understanding of how endogenous peptides regulate a variety of important biological processes. One neuropeptide that is demonstrating a number of important modulatory roles in the central nervous system (CNS) is neuropeptide S (NPS). NPS and its receptor (NPSR) was originally identified in 2002 by Sato et al.,[1] but Xu and colleagues initiated the research to delineate the in vivo role(s) of NPS in 2004.[2] NPS is a 20 amino acid peptide that functions as an agonist through activation of G_q or G_s protein coupled pathways.[2] Defining both receptor and peptide localization in the CNS provided the first indications of NPS function. In situ hybridization showed that NPSR mRNA was expressed widely throughout the CNS.[3] However, peptide precursor mRNA was limited to the locus ceruleus (LC) area and the parabrachial nucleus of the brainstem.[4] Based on these observations, NPS was hypothesized to be involved in a number of CNS functions.

The human NPSR has two splice variants with a number of polymorphisms. One that has been well characterized occurs at position 107 and generates two variants of the receptor that differ significantly in their pharmacology[5] and have been linked to panic disorder[6,7] and fear processing.[8] Since the discovery of NPS in 2002, modulation of the NPS system has also been linked to anxiety,[9,2,10,11] sleeping disorders,[2,12] asthma,[13] obesity,[14,15] PTSD,[16,17] and importantly, substance abuse.[18−21] NPSR activation has been shown to modulate reward circuits and is expressed in brain areas associated with reward processing such as the ventral tegmental area (VTA), amygdala and substantia nigra.[4] Microdialysis studies have demonstrated that central NPS administration stimulates dopamine release in the medial prefrontal cortex,[22] and local intra-VTA microinjections of NPS enhance dopamine release in the nucleus accumbens.[23] The latter study specifically links NPS to the mesolimbic dopamine system, which is presumed to be a major neuronal pathway modulating reward. NPS has also been shown to increase cocaine self-administration in a corticotrophin releasing factor (CRF) dependent manner.[24]

Blockade of the NPSR using small molecule antagonists attenuates both drug-seeking and drug-taking behaviors.[20,25] The prototypical NPS antagonist SHA-68 (**1**) shows selective antagonism at the human NPSR at an in vitro potency of 13.7 nM and has been reported to prevent the arousal promoting and anxiolytic-like effects elicited by NPS.[26,27] More recently it was found that in rats, peripheral administration of **1** reduced
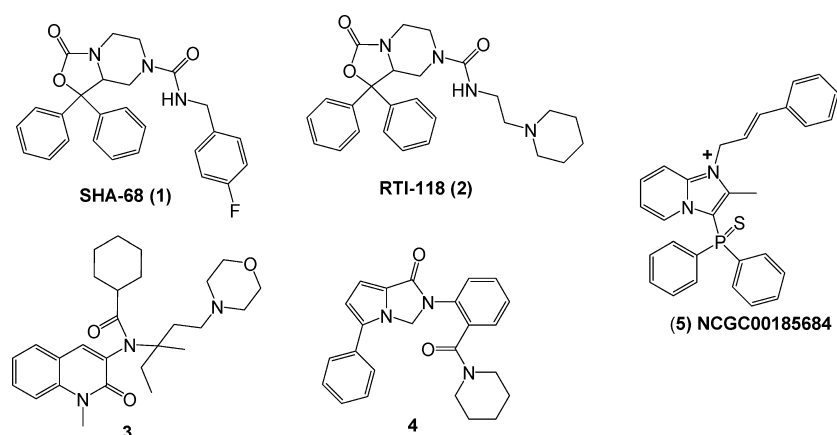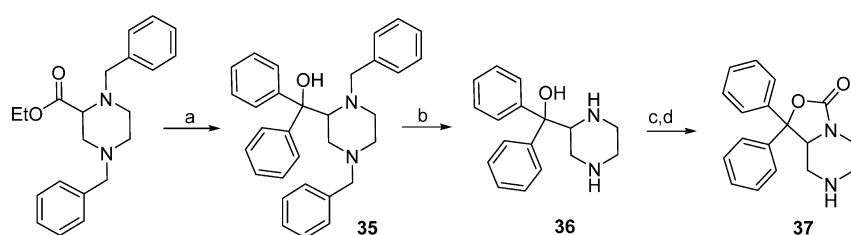
Figure 1. Representative classes of NPS antagonists.

Scheme 1. Synthesis of Key Intermediate 37[a]

[a]Reagents and conditions: (a) PhLi, THF, −78 °C; (b) H_2 (46 psi), 10% Pd/C, 5% Pd/BaSO$_4$, EtOH; (c) Boc$_2$O, DMAP, NEt$_3$, THF; (d) TFA, DCM.

conditioned reinstatement of cocaine seeking in two studies,[25,20] yet it was found in one study to reduce cocaine self-administration but only with a concomitant reduction in food self-administration at doses up to 30 mg/kg, ip.[20]

Several other small molecule NPSR antagonists have recently been reported, primarily by several large pharmaceutical companies, most of which are yet to be evaluated in vivo. For instance, Merck Research Laboratories identified two scaffolds through high-throughput screening (HTS) that have high potency at the NPSR using a calcium mobilization assay. Quinolinone scaffold **3** had a potency of 18 nM and was found to have acceptable drug-like properties,[28] and the second series contained a tricyclic imidazole that displayed potencies in the 40–80 nM range.[29] In addition, GlaxoSmithKline identified a highly potent naphthopyranopyrimidine scaffold **4**.[30] Finally, another small molecule scaffold identified to date is NCGC00185684 (**5**), which resulted from an NIH Molecular Libraries HT screen.[31] Compound **5** has good potency in both calcium mobilization and cAMP assays at 1 and 45 nM, respectively, and has recently been shown to reduce operant self-administration of alcohol at 1 mg/kg ip.

Our laboratory has developed a series of NPS antagonists based on the structure of SHA-68 and has recently demonstrated that one of these compounds, RTI-118 (**2**, Figure 1) blocks cocaine self-administration, cue, stress, and drug induced reinstatement.[20] Interestingly, compounds **1** and **2** both reduced cue-induced reinstatement of extinguished cocaine self-administration in rats at similar doses (30 mg/kg), yet only **2** selectively blocked cocaine self-administration. Although at a higher dose of 50 mg/kg **1** was able to reduce cocaine self-administration, it also decreased food-maintained responding, suggesting a nonselective impairment of operant behavior. However, **2** was able to selectively reduce cocaine

self-administration at lower doses (10–20 mg/kg, ip) without affecting food self-administration. These results indicate that **2** has better in vivo efficacy for reducing cocaine self-administration compared with **1**. Interestingly, **2** (K_e = 109 nM) has roughly 8-fold reduction in antagonist potency versus **1** (13.9 nM) at the NPSR 107I variant when tested in the calcium mobilization assay.[27] One distinct structural difference between these compounds is the ability of **2** to be partially ionized at physiological pH and thus more water-soluble. Therefore, the observed difference in efficacy between the two antagonists could be due to differences in drug-like properties.

We herein report the further evaluation of RTI-118, including the in vitro and in vivo pharmacokinetic properties, as well as additional SAR studies in an effort to shed light on the possible mechanisms for the behavioral differences between the two series. Although five structural classes of small molecule NPS antagonists are currently known, a comprehensive knowledge of the structure–activity relationships is still somewhat limited and a more detailed understanding of the molecular requirements for antagonist activity at the NPSR is required. The continued development of small molecules having improved potency and better drug-like properties than **1** may enable a better understanding of the NPS receptor system. In this study, we describe steps toward the development of a comprehensive pharmacophore with a bias toward increasing aqueous solubility and drug-like properties. Continued development of molecules that have improved drug-like properties will enable more detailed studies of the NPSR as an emerging target for a variety of CNS related disorders.

■ CHEMISTRY

The synthesis of all target compounds in this study was based on modifications to a central core scaffold. The synthesis of

Scheme 2. Synthesis of Target Molecules Derived from Isocyanate or Acid Chloride Addition[a]
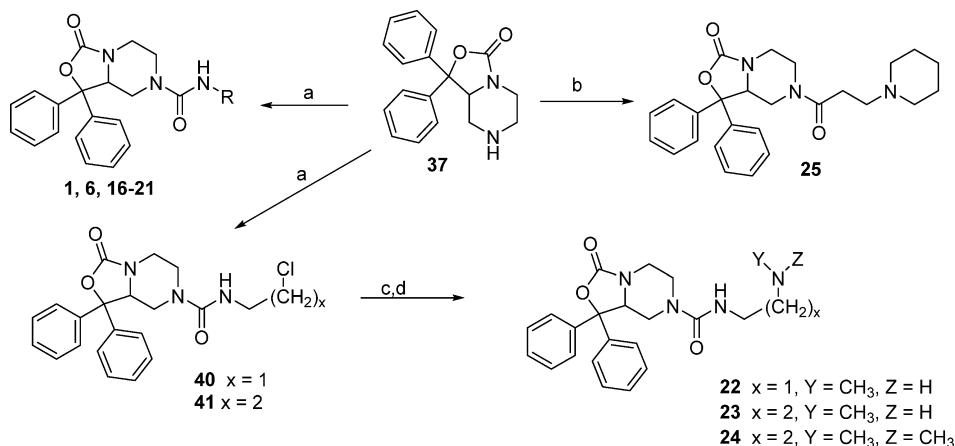
[a]Reagents and Conditions: (a) *R*-isocyanate, CH_2Cl_2, rt; (b) acid chloride, TEA, 0 °C; (c) CH_3NH_2, DMF, $KHCO_3$, rt; (d) $(CH_3)_2NH$, DMF, $KHCO_3$, rt.

Scheme 3. Preparation of Target Molecules Using Triphosgene Conditions[a]
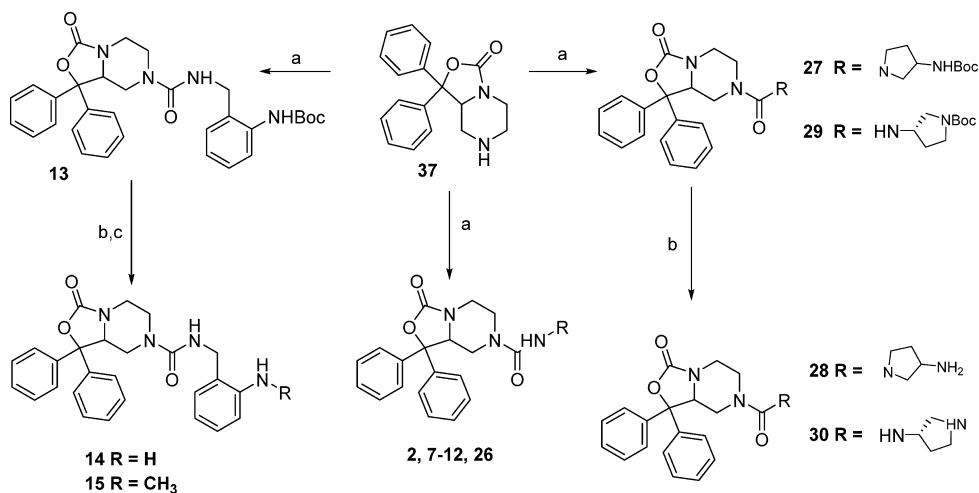
[a]Reagents and conditions: (a) *R*-amine, $(CCl_3O)_2CO$, TEA, THF, 0 °C to rt; (b) TFA, DCM; (c) HCOH, $NaH(OAc)_3$, 1,2-DCE.

Scheme 4. Identification of the Active Enantiomer of Key Intermediate 37[a]

38a
Camphor sulfonic acid salt
Sent for X-Ray analysis

31 Inactive isomer
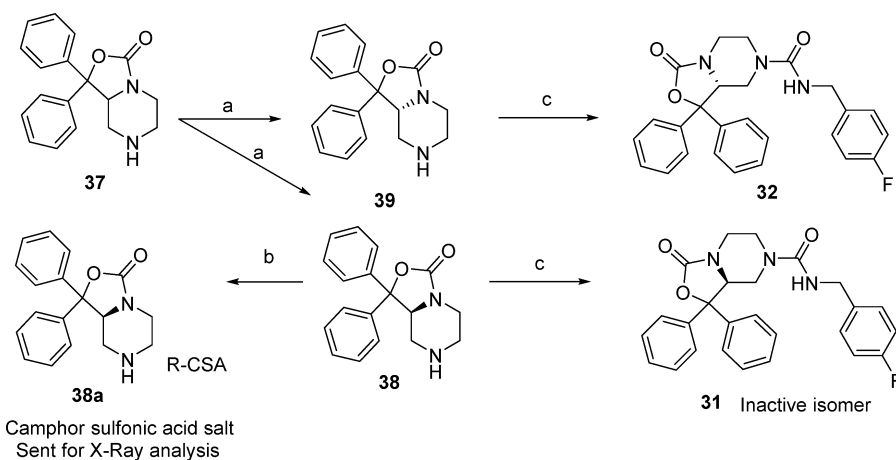
[a]Reagents and Conditions: (a) chiral HPLC; b) *R*-camphorsulfonic acid, MeOH; (c) 4-fluorobenzyl isocyanate.

core scaffold **37** was initiated through the condensation of 2 equiv of phenyl lithium with commercially available ethyl 1,4-

dibenzylpiperazine-2-carboxylate (Scheme 1). The resulting alcohol **35** was debenzylated using 5% palladium on barium

sulfate in ethanol to afford piperazine **36**. Cyclization of **36** was accomplished using *tert*-butyl dicarbonate, triethylamine, and dimethylaminopyridine in tetrahydrofuran.[32] This reaction required at least 1 equiv of dimethylaminopyridine to provide clean product. The resulting cyclic *tert*-butyl carbamate intermediate was deprotected with trifluoroacetic acid in dichloromethane to provide core scaffold **37** in good overall yield.

One of the primary goals of this research was to identify substituents that would confer improved aqueous solubility. Rapid condensation of a number of commercially available isocyanates with core scaffold **37** in dichloromethane provided compounds **1**, **6**, **16−21**, **40**, and **41** in good yield (Scheme 2). Displacement of the alkyl chlorides **40** and **41** with potassium carbonate, methyl amine, or dimethyl amine in dimethylformamide provided target molecules **22−24**, respectively, in moderate yield. Condensation of 3-(piperidin-1-yl)propanoic acid chloride with core scaffold **37** provided amide analog **25** in excellent yield.

Additional analogs containing basic amines were synthesized using a general method that incorporated the appropriate amine, triphosgene, and triethylamine in tetrahydrofuran. Compounds **2**, **7−13**, and **26** were prepared from **37** using triphosgene, triethylamine, and piperidine ethyl amine, alternately substituted pyridine methyl amines, alternately substituted pyridine ethyl amines, *tert*-butyl 2-(aminomethyl)-phenylcarbamate, and 1-methylpiperidin-4-amine, respectively (Scheme 3). Deprotection of **13** using trifluoroacetic acid in dichloromethane provided **14**. Reductive amination using sodium triacetoxyborohydride in 1,2-dichloroethane with 1 equiv of formaldehyde afforded a mixture of mono and dialkylated products from which **15** was isolated. Target compounds **27−30** were obtained using analogous methods to that described for compound **14**.

The identification of the active enantiomer of core scaffold **37** was performed using a combination of chiral HPLC and X-ray crystallography. Racemic **37** was subjected to chiral HPLC to afford enantiomers **38** and **39** (Scheme 4). The *R*-camphorsulfonic acid salt of **38** was prepared from *R*-camphorsulfonic acid in methanol. The resulting salt **38a** was subjected to X-ray analysis, and the chirality was determined to be *S* (Figure 2). Compounds **31** and **32** were then prepared from **38** and **39**, respectively, using 4-fluorobenzyl isocyanate in tetrahydrofuran. Compounds **33** and **34** were isolated via separation of **2** by chiral HPLC.

■ RESULTS AND DISCUSSION

One of the prototypical NPSR antagonists, SHA-68 (**1**), has been studied in a number of in vivo behavioral and in vitro biological assay systems. Pharmacokinetic studies have been performed on **1** and indicate that a significant component of the ip dose enters the CNS,[26] yet it behaves differently from **2** in vivo.[20] In order to provide a potential basis for this discrepancy, the aqueous solubility of **1** and **2** was evaluated. Aqueous solubility for **2** improved by a factor of 4200 at pH 3 and 3600 at pH 7 compared with **1** as determined by filtration through a 0.4 μm polycarbonate membrane in aqueous buffer (Millipore MultiScreen PCF 96 well filter plate).[33] Solubility at pH 3 and 7 for compound **1** is 0.01 and 0.01 μM and that for compound **2** is 42 and 36 μM, respectively. The enhanced solubility of **2** compared with **1** is quite striking and suggests the in vivo differences between **1** and **2** may be related to drug-like properties. Analogs that retain this property and have
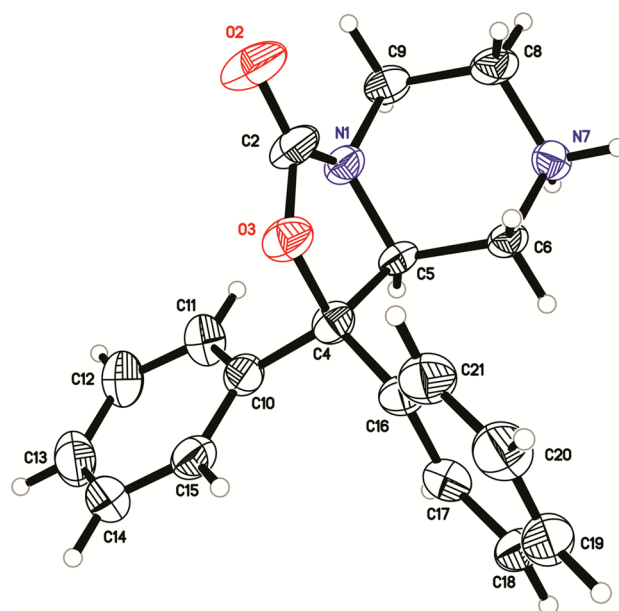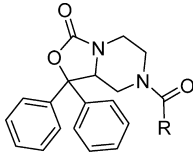

Figure 2. X-ray structure of the inactive enantiomer **38a**.

improved potency will provide additional tools to study the NPSR.

Considering the challenges of formulation and drug delivery for analogs like **1**, our laboratory set out to interrogate the tolerances to scaffold modification with the goal of improving aqueous solubility and receptor potency. Compounds were analyzed for agonist activity, and when they displayed no intrinsic activity, antagonist activity at the NPSR was measured using a functional calcium mobilization assay in stably transfected CHO-K1 cells. Each clone individually expressed one of the two predominant polymorphisms, 107I or 107N. The apparent constant K_e was determined by running EC_{50} curves of the agonist, NPS, with and without the test compounds to measure the rightward shift of the agonist curve. In keeping with literature reports, most compounds were more potent at the 107I variant of the NPSR ranging from 5.5-fold more potent to 0.59-fold. On average compounds were 1−2-fold more potent at the 107I variant. K_e values throughout the results section refer to results obtained using the 107I construct unless specifically noted.

The benzyl urea functions of **1** and **6** have previously been shown as preferred substituents for antagonist potency.[27] Based on this information, we introduced a series of benzylpyridines and pyridinylethyl ureas to enhance solubility. Substitution of **1** with a 2-pyridyl (**7**) reduced potency by 19-fold, while both the 3-pyridyl (**8**) and 4-pyridyl (**9**) also displayed a 19- and 30-fold reduction in potency, respectively, versus **1** (Table 1). This suggests that either increased polarity or electron density is not tolerated at this position. Elongation of the linker to ethyl further reduced antagonist potency. Compounds **10−12** had respective potencies of 945, 579, and 1157 nM as antagonists. In another attempt to provide compounds that could remain protonated in a suitable in vivo formulation, 2-aminobenzyl analogs were evaluated. N-Boc protected **13** had a limited effect on potency suggesting that this position could be modified with a variety of substituents and retain activity. Deprotection of **13** afforded free amine **14** (32 nM) that was only 2-fold reduced in activity from **1**. Monomethylation provided **15** having a K_e of 90 nM. Based on the data from Table 1, it appears that the

Table 1. Potency of Benzyl Urea Analogs of SHA-68 (1) in CHOK1 Cells Expressing Human NPSR Isoforms 107I and 107N
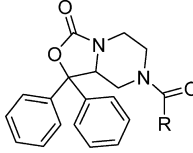

Compound	R	107I Ke (nM)	107N Ke (nM)	107N/107I
1		13.7 ± 4	52 ± 2	3.8
6		10 ± 2	47 ± 15	4.7
7		259 ± 64	292 ± 75	1.1
8		253 ± 58	331 ± 93	1.3
9		423 ± 41	442 ± 93	1.1
10		945 ± 253	725 ± 148	0.77
11		579 ± 110	481 ± 43	0.83
12		1157 ± 273	1482 ± 158	1.3
13		72 ± 21	201 ± 46	2.8
14		32 ± 15	87 ± 23	2.7
15		90 ± 35	414 ± 191	4.6

benzylic aryl ring is sensitive to alteration and that compounds with pyridyl substitution are not well tolerated.

Previous studies modifying the SHA-68 scaffold (**1**) indicated that benzylic substituents are preferred but that aliphatic substituents can also lead to analogs with moderate potency.[27] We thus set out to evaluate the size requirements for aliphatic substituents in place of the benzyl group on **1** (Table 2). Once the size limitations of the hypothetical binding site were determined, we could then evaluate tolerances to incorporation of solubilizing aliphatic amine groups. Progressive substitution with larger aliphatic moieties starting from ethyl (**16**, 2270 nM)

Table 2. Potency of Alkyl Substituted Urea Analogs of SHA-68 in CHOK1 Cells Expressing Human NPSR Isoforms 107I and 107N: Alkyl Substitution of the Urea to Determine Optimal Substituent Size
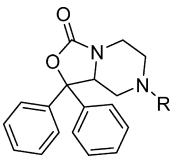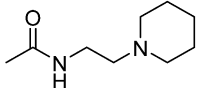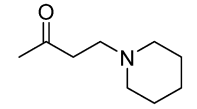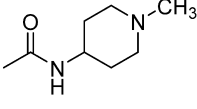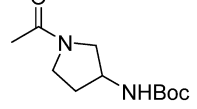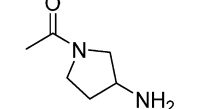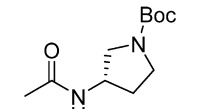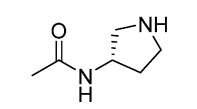

Compound	R	107I Ke (nM)	107N Ke (nM)	107N/107I
1		13.7 ± 4	52 ± 2	3.8
16		2270 ± 176	>5,000	-
17		953 ± 66	1047 ± 233	1.1
18		201 ± 25	879 ± 215	4.4
19		33 ± 3	54 ± 13	1.6
20		61 ± 16	94 ± 36	1.5
21		184 ± 36	382 ± 74	2.1
22		695 ± 23	804 ± 124	1.2
23		444 ± 46	1019 ± 232	2.3
24		782 ± 110	2070 ± 219	2.6

to isopropyl (**17**, 953 nM), to propyl (**18**, 201 nM), and then butyl (**19**, 33 nM) indicated that a benzylic moiety was not a requirement for optimal potency and alkyl substituted analogs could be prepared with comparable potency to **1**. Further elongation of the alkyl chain to pentyl (**20**, 61 nM) and hexyl (**21**, 184 nM) started to reduce potency from the optimal activity of butyl (**19**). This suggested that a lipophilic pocket of limited size accommodated aliphatic and benzylic groups. Once compound **19** was identified as the most potent alkyl analog, we set out to evaluate how incorporating amine groups would be tolerated. Compound **22** is an amino substituted analog of **19** but displays a 21-fold reduction in activity. Increasing the distance of amine from the urea by one carbon (**23**) slightly improved potency compared with **22**, but **23** remained 14-fold less potent than the *n*-butyl analog **22**. Methylation of **23** reduced activity to a K_e of 782 nM for dimethylated analog (**24**). This data indicates that substituted amino groups can be tolerated as in the case of **2** (K_e = 109 nM) but the disposition of the polar group is critical to activity.

Considering that compound **2** displayed moderate potency in earlier studies, we set out to define the receptor tolerances through altering the placement of ionizable amino groups within cyclic substituents (Table 3). Converting the urea functionality to an amide was performed to determine whether a series of commercial amides could be evaluated more rapidly. Replacement of the urea led to reduced potency for **25** having a K_e of 394 nM. This data supports earlier findings where

Table 3. Potency of Urea Analogs of SHA-68 in CHOK1 Cells Expressing Human NPSR Isoform 107I: Urea Substituents Designed to Enhance Aqueous Solubility
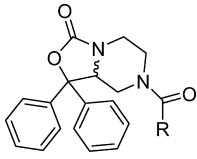

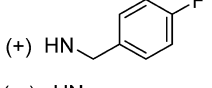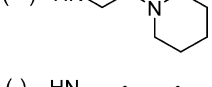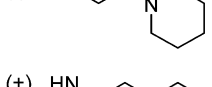| Compound	R	107I Ke (nM)	107N Ke (nM)	107N/107I
2		109 ± 23	490 ± 173	4.5
25		394 ± 105	456 ± 91	1.2
26		2091 ± 147	2338 ± 232	1.2
27		4121 ± 474	2424 ± 506	0.59
28		1461 ± 297	1659 ± 512	1.1
29		3384 ± 32	>5,000	-
30		510 ± 46	992 ± 108	1.9
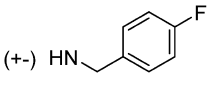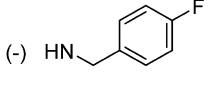
methylation of the urea nitrogen on **1** significantly reduced potency.[27] Compound **26** replaced the piperidinylethyl in **2** with an N-methylpiperidine that displayed significantly reduced activity (2091 nM) compared with **2**. Both the N-Boc protected and free amino pyrrolidines **27** and **28** also displayed reduced activity whereas pyrrolidine analogs **29** and **30** displayed potencies of 3384 nM and 510 nM, respectively. These data combined with results for the acyclic analogs **16−21** suggest that the receptor site prefers lipophilic substituents of specific size and that amides display reduced activity compared with ureas.

The importance of the chirality in **1** has been demonstrated where only the R isomer was active.[34] Similarly, only one bioactive enantiomer was isolated from the racemic mixture of NPS antagonist **3**.[28] The original chiral study of **1** utilized a multistep synthesis that relied on diastereomeric separation. Considering that one enantiomer is known to retain activity we set out to identify the active enantiomer of the synthetically common intermediate **37** that could be used to rapidly evaluate a number of chiral analogs with this class of compounds. The chiral intermediate described in this study (**37**) can be readily

appended with a large variety of substituents. The ability to further explore SAR using the known biologically active isomer of a synthetic intermediate is of significance. Thus, the intermediate amine **37** was separated into two isomers **38** and **39** using chiral HPLC. The chirality of these compounds was elucidated by preparing the R-camphorsulfonic acid salt of one of the isomers, **38**, and performing an X-ray study on the resulting salt **38a**. Based on this study **38a** had the S configuration. The corresponding 4-fluorobenzyl ureas were then prepared from **38** (S) and **39** (R), respectively, and tested in the calcium mobilization assay. Compound **32** showed a K_e of 5.1 nM, whereas **31** was inactive up to 5 μM, confirming that the R configuration is required for activity at the NPS receptor (Table 4). Similarly, the individual isomers of the piperidylethyl analog **33** and **34** were isolated, and only one isomer, **34**, displayed activity (36 nM) at the NPS receptor.

Table 4. Potency of Individual Enantiomers of Lead Compounds 1 and 2 in CHOK1 Cells Expressing Human NPSR Isoform 107I

Compound	R	107I Ke (nM)	107N Ke (nM)	107N/107I
1	(+−)	13.7 ± 4	52 ± 2	3.8
31	(−)	>5,000	75,000	-
32	(+)	5.1 ± 1.0	28 ± 3	5.5
2	(+−)	109 ± 23	490 ± 173	4.5
33	(−)	>5,000	75,000	-
34	(+)	36 ± 4	110 ± 41	3.1

In order to get a more detailed understanding of on-target effects in vivo, compound **34** was further evaluated for its pharmacokinetic properties (Figure 3). Following an ip dose, **34** was rapidly absorbed into systemic circulation, with peak plasma concentration observed at 15 min postdose. After a distribution phase, plasma concentrations declined with an apparent half-life of 33.9 min. Brain concentrations of **34** were measurable as early as 15 min postdose (the first sampling time point), with peak brain concentration observed at 15 min postdose. Compound **34** was eliminated from the brain with an apparent half-life of 143 min. The overall brain to plasma AUC ratio, as determined by AUC_{last} or AUC_{0-inf} ratio, was 0.14 or 0.29, respectively. This study provides a preliminary assessment of the brain penetration of **34** in mice after an ip dose of 5 mg/kg. At 90 min postdose, brain concentrations were approx-
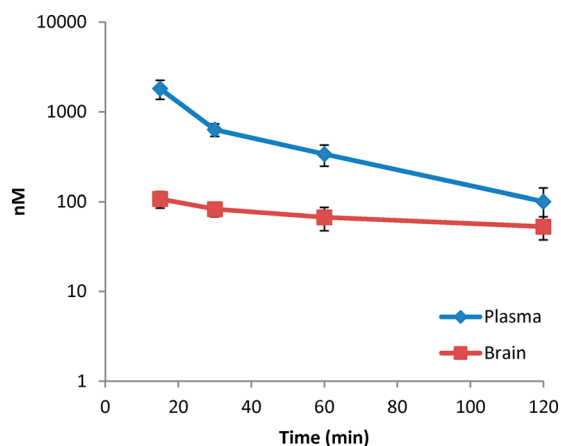
Figure 3. Pharmacokinetic analysis of compound **34** in brain and plasma; 5 mg/kg dose. Sample size, five animals per time point. Data points represent the mean, and error bars represent standard deviation.

imately 60 nM indicating sufficient brain penetration for NPS receptor modulation considering **34** has a K_e of 36 nM.

In Vivo Activity of 34. NPS is known to induce hyperlocomotion in mice after central administration.[2] To test whether this central effect of NPS can be antagonized by **34**, we recorded distance traveled at 5 min intervals over 90 min in mice that had received injections of vehicle or **34** (5 and 50 mg/kg ip) and subsequently received central administrations of either vehicle or 1 nmol of NPS icv. As shown in Figure 4, analysis of cumulative activity data revealed that injections of NPS + vehicle increased the cumulative distance traveled by the animals in a statistically significant manner. Compound **34** alone at 50 mg/kg did not modify per se the animal behavior compared with the control group ($p = 0.8738$, unpaired Student's t test). When challenged with NPS, **34** at a dose of 5 mg/kg resulted in a nonsignificant reduction (approximately 20%) of the distance traveled as compared with mice receiving NPS + vehicle injections ($p = 0.3515$, unpaired Student's t test). At the highest dose (50 mg/kg), **34** significantly attenuated (approximately 60%) the effects of 1 nmol of NPS, demonstrating that **34** (50 mg/kg) was effective at least partially antagonizing NPS-induced activity. Statistically significant effects were obtained with 50 mg/kg, although the antagonist did not fully prevent the effects elicited by the peptide. Together, these data demonstrate that **34** behaves as an NPSR antagonist in vivo and is centrally acting after peripheral administration.

■ CONCLUSIONS

A series of N-substituted diphenyltetrahydro-$1H$-oxazolo[3,4-α]pyrazin-3(5H)-ones have been synthesized and evaluated for antagonism of the NPS receptor system. The receptor tolerance to both size and polarity of these analogs at several locations were evaluated. The most potent antagonists possessed simple aliphatic ureas such as N-butyl (**19**) or ureas having basic amine containing substituents that were substituted with hydrophobic groups such as piperidinoethyl (**34**). Incorporation of protonatable nitrogen improved the aqueous solubility of this series while maintaining NPS receptor potency. Resolution of the key intermediate for the synthesis of these analogs and identification of the absolute configuration of the bioactive isomer now affords the opportunity to rapidly obtain a number of chiral analogs for future study. In vivo behavioral analysis of
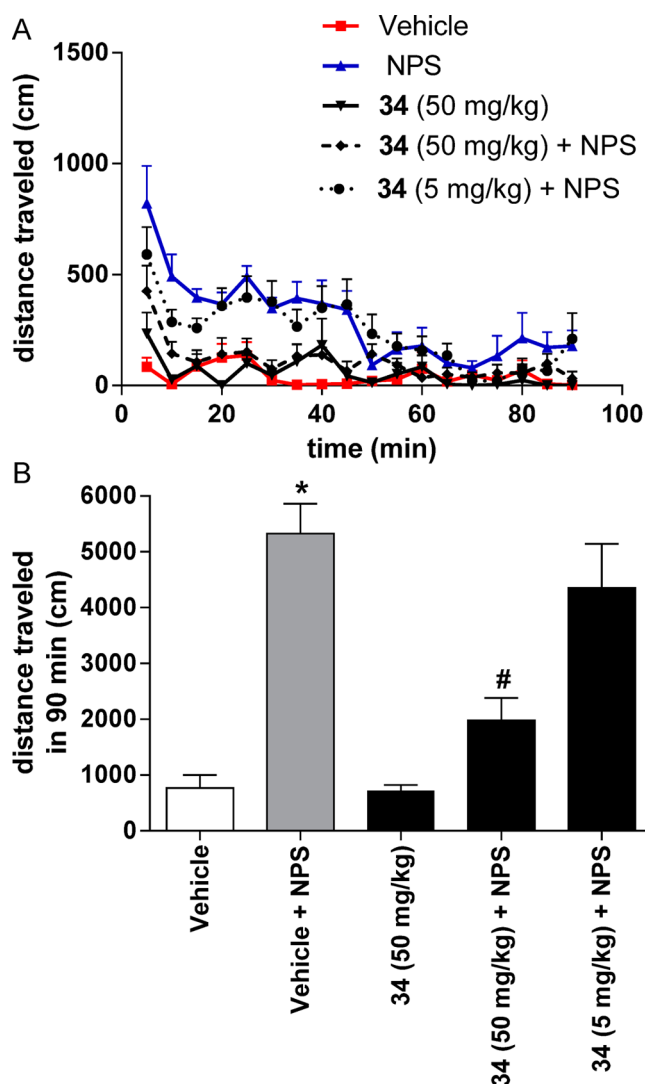
Figure 4. Effects of **34** on motor activity in mice. Mice had been habituated for 60 min before injection. Compound **34** was dissolved in 10% Cremophor EL (vehicle) and injected (ip) 10 min before NPS or vehicle (PBS, 0.1% BSA) were injected centrally (icv). Group sizes: Veh + Veh, $n = 8$; Veh + NPS, $n = 7$; **34** + PBS, $n = 7$; **34** (50 mg/kg) + NPS (1 nmole), $n = 8$; **34** (5 mg/kg) + NPS (1 nmole), $n = 9$. (A) Time course of the distance traveled over 90 min. (B) Total distance traveled during the 90 min observation period. *, $p < 0.001$, Veh + Veh versus Veh + NPS; #, $p < 0.001$ Veh + NPS versus NPS + **34** (50 mg/kg) (Students t test).

the most potent compound demonstrated the ability of one such compound (**34**) to significantly reduce NPS stimulated locomotor activity at a dose of 50 mg/kg. The analogs described in this study provide additional detail as to the requirements for biological activity at the NPSR and represent improved tools to study the NPSR in vivo. The improvement of aqueous solubility opens up possibilities not permitted with less soluble analogs such as iv administration and microinjections into discrete brain regions using an unmodified aqueous buffer system. Identification of additional analogs having improved properties could ultimately lead to pharmacotherapies to treat a variety of CNS disorders.

■ METHODS

General. All standard reagents were commercially available. Compounds were purified by column chromatography on a Teledyne Isco Rf chromatography unit and by HPLC on an Agilent-Varian HPLC system equipped with Prostar 210 dual pumps, a Prostar 335 diode UV detector and a SEDEX75 (SEDERE, Olivet, France) ELSD detector. The HPLC solvent system was binary, water containing 0.1% trifluoroacetic acid (TFA) and solvent B (acetonitrile containing 0−5% water and 0.1% TFA). A semipreparative Synergy Hydro RP 80A C18 column (4 μm, 250 mm × 21.2 mm column; Phenomenex) or a Gemini-NX RP C18 column (5 μm, 250 mm × 21.2 mm; Phenomenex) was used to purify final compounds at 15 mL/min using a linear gradient from 5% to 50% or 60% B over 30 min. The purity of final compounds was determined using an analytical Synergy Hydro RP80A C18 (4 μm, 250 mm × 4.60 mm column; Phenomenex) or a Gemini-NX C18 (5 μm, 250 mm × 4.6 mm; Phenomenex) with a linear gradient of 5%−95% solvent B over 20 or 30 min at a flow rate of 1 mL/min. Absorbance was monitored at 220 nm. Individual enantiomers were separated, and enantiomeric purity was determined using an analytical Chiralpak-IA column (4.6 mm × 250 mm) with isocratic conditions (hexanes/isopropanol 9/1 or methyl-*tert*-butylether/ethanol 8/2 or 95/5 containing 0.1% DEA; 1 mL/min). The molecular ion of final compounds was determined using a PE Sciex API 150 EX LC/MS system from PerkinElmer (San Jose, California). Reactions were monitored by thin-layer chromatography (TLC) carried out on precoated 60 Å 250 mm silica gel TLC plates with F-254 indicator visualized under UV light and developed using ceric ammonium molybdate. ^{1}H NMR spectra were recorded at 300 MHz on a Bruker Avance 300 Spectrospin instrument and are reported as follows: chemical shift δ in ppm (multiplicity, coupling constant (Hz), and integration). The following abbreviations were used to explain multiplicities: s = singlet, d = doublet, t = triplet, q = quartet, quin = quintet, m = multiplet, br = broad, dd = doublet of doublets, dt = doublet of triplets, ddd = doublet of doublets of doublets, ddt = doublet of doublet of triplets. Optical rotations were determined using a Rudolph Research Autopol III automatic polarimeter.

*N-(4-Fluorobenzyl)-3-oxo-1,1-diphenyltetrahydro-1H-oxazolo-[3,4-a]pyrazine-7(3H)-carboxamide (**1**).* To a solution of **37** (50 mg, 0.17 mmol) in CH$_2$Cl$_2$ (5 mL) at 0 °C under N$_2$ was added 1-fluoro-4-(isocyanatomethyl)benzene (143 μL, 0.170 mmol). The reaction mixture was stirred at room temperature for 2 h and concentrated, and the residue was purified by medium pressure column chromatography (12 g f SiO$_2$, 100% methylene chloride to 50% chloroform/methanol/ammonium hydroxide 80/20/1) followed by semipreparative HPLC to provide **1** as a white powder (29 mg, 30%). ^{1}H NMR (300 MHz, chloroform-*d*) δ ppm 2.17 (dd, *J* = 13.19, 11.30 Hz, 1 H), 2.83−3.00 (m, 1 H), 3.01−3.16 (m, 1 H), 3.63 (dd, *J* = 13.00, 1.70 Hz, 1 H), 3.86 (dd, *J* = 13.00, 2.45 Hz, 1 H), 4.03 (dd, *J* = 13.19, 2.26 Hz, 1 H), 4.26−4.49 (m, 3 H), 4.69−4.81 (m, 1 H), 6.95−7.09 (m, 1 H), 7.21−7.45 (m, 11 H), 7.47−7.56 (m, 2 H). ESI MS *m/z*: calcd for C$_{26}$H$_{24}$FN$_3$O$_3$ 445.49, found 446.7 (M + H)$^+$. HPLC (Synergy Hydro, 20 min) t_R = 19.47 min (>99%).

*3-Oxo-1,1-diphenyl-N-(2-(piperidin-1-yl)ethyl)tetrahydro-1H-oxazolo[3,4-a]pyrazine-7(3H)-carboxamide (**2**).* To a solution of **37** (0.5 g, 1.70 mmol) in THF (anhydrous, 70 mL) at 0 °C under N$_2$ was added triphosgene (0.17 g, 0.57 mmol), and the reaction mixture was allowed to stir at 0 °C for 5 min. To this mixture was added triethylamine (710 μL, 5.1 mmol), and the reaction was allowed to stir at 0 °C for 5 min. To this mixture was then added piperidine ethylamine (240 μL, 1.67 mmol) at 0 °C, and the reaction mixture was allowed to stir at 0 °C for 2 h and then warmed to room temperature. The resulting suspension was concentrated to dryness and taken up in CH$_2$Cl$_2$ (100 mL). The suspension was made basic with sat. aq. NaHCO$_3$ and extracted with CH$_2$Cl$_2$ (3 × 100 mL). The organic layers were washed with brine (50 mL), dried (MgSO$_4$), and concentrated. The residue was purified by column chromatography (12 g of SiO$_2$, 100% methylene chloride to 40% chloroform/methanol/ammonium hydroxide 80/20/1) provided **2** (470 mg, 62%) as a white solid. ^{1}H NMR (300 MHz, chloroform-*d*) δ ppm 1.48 (d, *J*

= 4.52 Hz, 2 H), 1.58 (m, *J* = 4.90 Hz, 4 H), 2.18 (dd, *J* = 13.19, 11.30 Hz, 1 H), 2.37−2.55 (m, 6 H), 2.84 (td, *J* = 12.72, 3.58 Hz, 1 H), 3.08 (td, *J* = 12.62, 3.77 Hz, 1 H), 3.31 (quin, *J* = 5.18 Hz, 2 H), 3.73−3.97 (m, 3 H), 4.43 (dd, *J* = 11.11, 3.58 Hz, 1 H), 5.47−5.74 (m, 1 H), 7.28−7.45 (m, 8 H), 7.49−7.58 (m, 2 H). ESI HRMS *m/z*: calcd for C$_{26}$H$_{32}$N$_4$O$_3$ 448.57, found 449.25 (M + H)$^+$. HPLC (Synergy Hydro, 20 min) t_R = 15.23 min (>99%).

*N-Benzyl-3-oxo-1,1-diphenyltetrahydro-1H-oxazolo[3,4-a]-pyrazine-7(3H)-carboxamide (**6**).* An analogous procedure to that described for **1** using benzyl isocyanate provided **6** as a white solid (31 mg, 86%). ^{1}H NMR (300 MHz, chloroform-*d*) δ ppm 2.10−2.22 (m, 1 H), 2.81−2.95 (m, 1 H), 3.00−3.12 (m, 1 H), 3.59−3.70 (m, 1 H), 3.82 (dd, *J* = 13.00, 3.20 Hz, 1 H), 4.03 (dt, *J* = 13.28, 1.84 Hz, 1 H), 4.31−4.49 (m, 3 H), 4.89 (br s, 1 H), 7.24−7.42 (m, 13 H), 7.47−7.54 (m, 2 H). ESI HRMS *m/z*: calcd for C$_{26}$H$_{25}$N$_3$O$_3$ 427.19, found 450.18 (C$_{26}$H$_{25}$N$_3$O$_3$ +Na)$^+$.

*3-Oxo-1,1-diphenyl-N-(pyridin-2-ylmethyl)tetrahydro-1H-oxazolo[3,4-α]pyrazine-7(3H)-carboxamide (**7**).* An analogous procedure to that described for **2** using pyridin-2-ylmethanamine provided **7** as a white powder (42 mg, 58%). ^{1}H NMR (300 MHz, chloroform-*d*) δ ppm 2.21 (dd, *J* = 13.19, 11.30 Hz, 1 H), 2.96 (dd, *J* = 13.56, 3.77 Hz, 1 H), 3.10 (dd, *J* = 13.19, 3.77 Hz, 1 H), 3.78−3.93 (m, 2 H), 4.04 (dd, *J* = 13.37, 2.45 Hz, 1 H), 4.44 (dd, *J* = 11.30, 3.77 Hz, 1 H), 4.48−4.68 (m, 2 H), 5.95−6.09 (m, 1 H), 7.21 (dd, *J* = 7.16, 5.27 Hz, 1 H), 7.27−7.44 (m, 9 H), 7.49−7.60 (m, 2 H), 7.67 (td, *J* = 7.63, 1.70 Hz, 1 H), 8.52 (d, *J* = 4.90 Hz, 1 H). ESI MS *m/z*: calcd for C$_{25}$H$_{24}$N$_4$O$_3$ 428.49, found 427.6 (M − H)$^-$, 429.2 (M + H)$^+$, 451.5 (M + Na)$^+$. HPLC (Synergy Hydro, 20 min) t_R = 14.61 min (95.0%).

*3-Oxo-1,1-diphenyl-N-(pyridin-3-ylmethyl)tetrahydro-1H-oxazolo[3,4-α]pyrazine-7(3H)-carboxamide (**8**).* An analogous procedure to that described for **2** using pyridin-3-ylmethanamine provided **8** as white powder (52 mg, 71%). ^{1}H NMR (300 MHz, chloroform-*d*) δ ppm 2.19 (dd, *J* = 13.56, 11.30 Hz, 1 H), 2.95 (dd, *J* = 13.00, 3.20 Hz, 1 H), 3.03−3.15 (m, 1 H), 3.61−3.70 (m, 1 H), 3.82−3.93 (m, 1 H), 3.95−4.05 (m, 1 H), 4.34−4.51 (m, 2 H), 4.83 (br s, 1 H), 7.22−7.43 (m, 10 H), 7.48−7.55 (m, 2 H), 7.64 (d, *J* = 7.16 Hz, 1 H), 8.51−8.57 (m, 1 H). ESI MS *m/z*: calcd for C$_{25}$H$_{24}$N$_4$O$_3$ 428.49, found 427.4 (M − H)$^-$, 429.0 (M + H)$^+$, 451.3 (M + Na)$^+$. HPLC (Synergy Hydro, 20 min) t_R = 14.20 min (93.4%).

*3-Oxo-1,1-diphenyl-N-(pyridin-4-ylmethyl)tetrahydro-1H-oxazolo[3,4-α]pyrazine-7(3H)-carboxamide (**9**).* An analogous procedure to that described for **2** using pyridin-4-ylmethanamine provided **9** as a white powder (47 mg, 65%). ^{1}H NMR (300 MHz, chloroform-*d*) δ ppm 2.20 (dd, *J* = 13.56, 11.30 Hz, 1 H), 2.89−3.02 (m, 1 H), 3.03−3.18 (m, 1 H), 3.62−3.75 (m, 1 H), 3.82−3.94 (m, 1 H), 4.02 (ddd, *J* = 13.38, 3.58, 1.51 Hz, 1 H), 4.31−4.51 (m, 3 H), 5.01 (br s, 1 H), 7.13−7.23 (m, 2 H), 7.24−7.44 (m, 8 H), 7.47−7.58 (m, 2 H), 8.49−8.64 (m, 2 H). ESI MS *m/z*: calcd for C$_{25}$H$_{24}$N$_4$O$_3$ 428.49, found 429.3 (M + H)$^+$; 451.4 (M + Na)$^+$, 427.5 (M − H)$^-$, HPLC (Synergy Hydro, 20 min) t_R = 14.04 min (94.1%).

*3-Oxo-1,1-diphenyl-N-(2-(pyridin-2-yl)ethyl)tetrahydro-1H-oxazolo[3,4-α]pyrazine-7(3H)-carboxamide (**10**).* An analogous procedure to that described for **2** using 2-(pyridin-2-yl)ethanamine provided **10** as white powder (50 mg, 66%). ^{1}H NMR (300 MHz, chloroform-*d*) δ ppm 2.17 (dd, *J* = 13.19, 11.30 Hz, 1 H), 2.84 (td, *J* = 12.81, 3.39 Hz, 1 H), 2.93−3.11 (m, 3 H), 3.55−3.66 (m, 2 H), 3.72−3.87 (m, 2 H), 3.89−4.00 (m, 1 H), 4.39 (dd, *J* = 11.11, 3.58 Hz, 1 H), 6.30 (t, *J* = 4.90 Hz, 1 H), 7.12−7.21 (m, 2 H), 7.23−7.42 (m, 8 H), 7.46−7.55 (m, 2 H), 7.63 (td, *J* = 7.72, 1.88 Hz, 1 H), 8.43 (dt, *J* = 4.62, 1.46 Hz, 1 H). ESI MS *m/z*: calcd for C$_{26}$H$_{26}$N$_4$O$_3$ 442.52, found 443.4 (M + H)$^+$, 441.4 (M − H)$^-$. HPLC (Synergy Hydro, 20 min) t_R = 14.76 min (97.8%).

*3-Oxo-1,1-diphenyl-N-(2-(pyridin-3-yl)ethyl)tetrahydro-1H-oxazolo[3,4-α]pyrazine-7(3H)-carboxamide (**11**).* An analogous procedure to that described for **2** using 2-(pyridin-3-yl)ethanamine provided **11** as a white powder (28 mg, 37%). ^{1}H NMR (300 MHz, chloroform-*d*) δ ppm 2.14 (dd, *J* = 13.19, 11.30 Hz, 1 H), 2.78−2.95 (m, 3 H), 3.02 (td, *J* = 12.72, 3.58 Hz, 1 H), 3.34−3.53 (m, 2 H), 3.60 (d, *J* = 12.81 Hz, 1 H), 3.81 (dd, *J* = 12.81, 2.64 Hz, 1 H), 3.94 (dd, *J* = 13.19, 3.39 Hz, 1 H), 4.39 (dd, *J* = 11.30, 3.77 Hz, 1 H), 7.17−7.44

(m, 9 H), 7.46–7.56 (m, 3 H), 8.35–8.50 (m, 2 H). ESI MS m/z: calcd for $C_{26}H_{26}N_4O_3$ 442.52, found 441.3 (M − H)$^-$, 443.5 (M + H)$^+$, 465.4 (M + Na)$^+$. HPLC (Synergy Hydro, 20 min) t_R = 14.59 min (97.9%).

3-Oxo-1,1-diphenyl-N-(2-(pyridin-4-yl)ethyl)tetrahydro-1H-oxazolo[3,4-α]pyrazine-7(3H)-carboxamide (12). An analogous procedure to that described for **2** using 2-(pyridin-4-yl)ethanamine provided **12** as a white powder (55 mg, 72%). ^{1}H NMR (300 MHz, chloroform-d) δ ppm 2.09–2.20 (m, 1 H), 2.78–2.91 (m, 3 H), 3.01 (td, J = 12.72, 3.20 Hz, 1 H), 3.40–3.57 (m, 2 H), 3.59–3.71 (m, 1 H), 3.78 (d, J = 13.19 Hz, 1 H), 3.96 (dd, J = 13.37, 2.83 Hz, 1 H), 4.39 (dd, J = 11.11, 3.58 Hz, 1 H), 7.04–7.11 (m, 2 H), 7.19–7.44 (m, 8 H), 7.44–7.53 (m, 2 H), 8.40 (d, J = 4.33, 1.70 Hz, 2 H). ESI MS m/z: calcd for $C_{26}H_{26}N_4O_3$ 442.52, found 441.5 (M − H)$^-$, 443.5 (M + H)$^+$, 465.3 (M + Na)$^+$. HPLC (Synergy Hydro, 20 min) t_R = 14.55 min (90.6%).

tert-Butyl-2-((3-oxo-1,1-diphenylhexahydro-1H-oxazolo[3,4-a]pyrazine-7-carboxamido)methyl)-phenylcarbamate (13). An analogous procedure to that described for **2** using *tert*-butyl-2-(aminomethyl)phenylcarbamate provided **13** as a viscous oil (75 mg, 44%). ^{1}H NMR (300 MHz, chloroform-d) δ ppm 1.50 (s, 9 H), 2.14 (dd, J = 13.37, 11.11 Hz, 1 H), 2.73–2.89 (m, 1 H), 2.93–3.09 (m, 1 H), 3.66–3.85 (m, 2 H), 3.91–4.02 (m, 1 H), 4.29 (d, J = 5.65 Hz, 1 H), 4.34–4.48 (m, 2 H), 5.44 (s, 1 H), 7.04 (dd, J = 7.54, 1.13 Hz, 1 H), 7.21–7.42 (m, 10 H), 7.44–7.54 (m, 2 H), 7.70 (d, J = 7.91 Hz, 1 H), 8.15 (s, 1 H). ESI MS m/z: calcd for $C_{31}H_{34}N_4O_5$ 542.25, found 565.3 (M + 23)$^+$.

N-(2-Aminobenzyl)-3-oxo-1,1-diphenyltetrahydro-1H-oxazolo-[3,4-a]pyrazine-7(3H)-carboxamide (14). Compound **13** (73 mg, 0.13 mmol) was dissolved in CH_2Cl_2 (10 mL) at 0 °C. Anhydrous TFA (5 mL) was then added to the solution and allowed to stir at rt for 2 h. The resulting solution was basified with sat. aq. NaHCO$_3$ to pH 11 and extracted with CH_2Cl_2 (3 × 20 mL). The organic extracts were combined, dried with MgSO$_4$, and concentrated to provide a viscous oil. The oil was purified using medium pressure column chromatography (12 g of SiO$_2$, 100% methylene chloride to 50% chloroform/methanol/ammonium hydroxide 80/20/1) to provide **14** as a viscous oil (59 mg, 99%). ^{1}H NMR (300 MHz, chloroform-d) δ ppm 2.07–2.21 (m, 1 H), 2.79 (td, J = 12.81, 3.77 Hz, 1 H), 2.92–3.13 (m, 1 H), 3.61–3.81 (m, 3 H), 3.93 (dd, J = 13.19, 3.01 Hz, 3 H), 4.25–4.50 (m, 4 H), 5.06 (br s, 1 H), 6.61–6.72 (m, 2 H), 6.99–7.14 (m, 2 H), 7.23–7.40 (m, 8 H), 7.44–7.52 (m, 2 H). ESI MS m/z: calcd for $C_{26}H_{26}N_4O_3$ 442.20, found 443.5 (M + H)$^+$.

N-(2-(Methylamino)benzyl)-3-oxo-1,1-diphenyltetrahydro-1H-oxazolo[3,4-a]pyrazine-7(3H)-carboxamide (15). To a solution of **14** (55 mg, 0.124 mmol) in 1,2-dichloroethane (5 mL) was added formaldehyde (37% solution in water, 37 μL, 0.50 mmol) and sodium triacetoxyborohydride (105 mg, 0.50 mmol). The reaction mixture was stirred at room temperature for 1 h and then quenched with NaHCO$_3$ (sat. aq. solution; 10 mL), and the aqueous layer was washed with methylene chloride (2 × 10 mL). The organic layer was separated, washed with brine (5 mL), dried (MgSO$_4$), and concentrated under reduced pressure to provide an oil. The oil was purified by column chromatography (12 g of SiO$_2$, 100% methylene chloride to 50% chloroform/methanol/ammonium hydroxide 80/20/1) to provide **15** as a white solid (6 mg, 5%). ^{1}H NMR (300 MHz, DMSO-d_6) δ ppm 2.10–2.25 (m, 1 H), 2.54 (s, 1 H), 2.79 (s, 3 H), 3.19–3.31 (m, 1 H), 3.37–3.47 (m, 1 H), 3.50–3.70 (m, 2 H), 4.32 (d, J = 6.40 Hz, 2 H), 4.43 (s, 2 H), 4.67–4.79 (m, 1 H), 6.66–6.78 (m, 2 H), 6.95–7.14 (m, 2 H), 7.25–7.48 (m, 8 H), 7.54–7.65 (m, 2 H). ^{1}H NMR (300 MHz, chloroform-d) δ ppm 2.24 (dd, J = 13.56, 11.30 Hz, 1 H), 2.88 (s, 3 H), 2.91–3.05 (m, 1 H), 3.05–3.23 (m, 1 H), 3.67 (d, J = 12.43 Hz, 2 H), 3.85 (dd, J = 13.00, 2.83 Hz, 1 H), 4.23–4.32 (m, 1 H), 4.38–4.46 (m, 1 H), 4.47–4.61 (m, 3 H), 6.71–6.86 (m, 2 H), 6.96 (d, J = 6.40 Hz, 1 H), 7.11–7.21 (m, 1 H), 7.27–7.42 (m, 8 H), 7.47–7.56 (m, 2 H). ESI MS m/z: calcd for $C_{27}H_{28}N_4O_3$ 456.54, found 458.3 (M + H)$^+$.

N-Ethyl-3-oxo-1,1-diphenyltetrahydro-1H-oxazolo[3,4-a]pyrazine-7(3H)-carboxamide (16). An analogous procedure to that described for **1** using ethylisocyanate provided **16** as viscous oil (160

mg, 93%). ^{1}H NMR (300 MHz, chloroform-d) δ ppm 1.13 (t, J = 7.16 Hz, 3 H), 2.07–2.20 (m, 1 H), 2.81–2.96 (m, 1 H), 3.07 (td, J = 12.72, 3.58 Hz, 1 H), 3.19–3.35 (m, 2 H), 3.58–3.69 (m, 1 H), 3.84 (dd, J = 13.00, 2.45 Hz, 1 H), 4.00 (ddd, J = 13.28, 3.49, 1.32 Hz, 1 H), 4.42 (dd, J = 11.30, 3.39 Hz, 1 H), 4.50–4.58 (m, 1 H), 7.25–7.42 (m, 8 H), 7.47–7.54 (m, 2 H). ESI HRMS m/z: calcd for $C_{21}H_{23}N_3O_3$ 365.17, found 388.16 (M + Na)$^+$.

N-Isopropyl-3-oxo-1,1-diphenyltetrahydro-1H-oxazolo[3,4-a]-pyrazine-7(3H)-carboxamide (17). An analogous procedure to that described for **1** using *i*-propylisocyanate provided **17** as a viscous oil (166 mg, 93%). ^{1}H NMR (300 MHz, chloroform-d) δ ppm 1.10–1.21 (m, 6 H), 2.02–2.18 (m, 1 H), 2.79–2.95 (m, 1 H), 3.07 (td, J = 12.62, 3.39 Hz, 1 H), 3.59 (dt, J = 13.19, 1.70 Hz, 1 H), 3.78–4.11 (m, 3 H), 4.33 (d, J = 7.16 Hz, 1 H), 4.42 (dd, J = 11.30, 3.77 Hz, 1 H), 7.25–7.44 (m, 8 H), 7.46–7.56 (m, 2 H). ESI HRMS m/z: calcd for $C_{22}H_{25}N_3O_3$ 379.19, found 402.18 (M + Na)$^+$.

3-Oxo-1,1-diphenyl-N-propyltetrahydro-1H-oxazolo[3,4-a]-pyrazine-7(3H)-carboxamide (18). An analogous procedure to that described for **1** using *n*-propylisocyanate provided **18** as a viscous oil (166 mg, 93%). ^{1}H NMR (300 MHz, chloroform-d) δ ppm 0.91 (t, J = 7.54 Hz, 3 H), 1.46–1.59 (m, 2 H), 2.07–2.20 (m, 1 H), 2.83–2.95 (m, 1 H), 3.07 (td, J = 12.62, 3.39 Hz, 1 H), 3.18 (tdd, J = 7.25, 7.25, 5.46, 1.88 Hz, 2 H), 3.63 (dt, J = 13.19, 1.88 Hz, 1 H), 3.84 (dd, J = 12.81, 2.64 Hz, 1 H), 4.01 (ddd, J = 13.28, 3.67, 1.51 Hz, 1 H), 4.42 (dd, J = 11.30, 3.39 Hz, 1 H), 4.55 (t, J = 5.46 Hz, 1 H), 7.23–7.44 (m, 8 H), 7.47–7.56 (m, 2 H). ESI HRMS m/z: calcd for $C_{22}H_{25}N_3O_3$ 379.19, found 402.18 (M + Na)$^+$.

N-Butyl-3-oxo-1,1-diphenyltetrahydro-1H-oxazolo[3,4-a]-pyrazine-7(3H)-carboxamide (19). An analogous procedure to that described for **1** using *n*-butylisocyanate provided **19** as a viscous oil (24 mg, 71%). ^{1}H NMR (300 MHz, chloroform-d) δ ppm 0.87–0.97 (m, 3 H), 1.30–1.40 (m, 2 H), 1.41–1.54 (m, 2 H), 2.07–2.19 (m, 1 H), 2.81–2.94 (m, 1 H), 3.07 (td, J = 12.62, 3.39 Hz, 1 H), 3.16–3.27 (m, 2 H), 3.59–3.69 (m, 1 H), 3.83 (dd, J = 13.00, 2.83 Hz, 1 H), 3.95–4.05 (m, 1 H), 4.41 (dd, J = 11.11, 3.58 Hz, 1 H), 4.61 (t, J = 5.27 Hz, 1 H), 7.23–7.44 (m, 8 H), 7.47–7.57 (m, 2 H). ESI HRMS m/z: calcd for $C_{23}H_{27}N_3O_3$ 393.21, found 416 0.19 (M + Na)$^+$.

3-Oxo-N-pentyl-1,1-diphenyltetrahydro-1H-oxazolo[3,4-a]-pyrazine-7(3H)-carboxamide (20). An analogous procedure to that described for **1** using *n*-pentylisocyanate provided **20** as viscous oil (39 mg, 64%). ^{1}H NMR (300 MHz, chloroform-d) δ ppm 0.81–0.98 (m, 3 H), 1.18–1.41 (m, 4 H), 1.49 (quin, J = 7.25 Hz, 2 H), 2.13 (dd, J = 13.19, 11.30 Hz, 1 H), 2.79–2.97 (m, 1 H), 3.07 (td, J = 12.62, 3.77 Hz, 1 H), 3.14–3.31 (m, 2 H), 3.56–3.72 (m, 1 H), 3.83 (dd, J = 13.19, 2.64 Hz, 1 H), 4.01 (ddd, J = 13.37, 3.58, 1.13 Hz, 1 H), 4.41 (dd, J = 11.30, 3.77 Hz, 1 H), 4.57 (t, J = 5.46 Hz, 1 H), 7.16–7.46 (m, 8 H), 7.47–7.61 (m, 2 H). ESI HRMS m/z: calcd for $C_{24}H_{29}N_3O_3$ 407.22, found 430.21 (M + Na)$^+$.

N-Hexyl-3-oxo-1,1-diphenyltetrahydro-1H-oxazolo[3,4-a]-pyrazine-7(3H)-carboxamide (21). An analogous procedure to that described for **1** using *n*-hexylisocyanate provided **21** as a viscous oil (39 mg, 61%). ^{1}H NMR (300 MHz, chloroform-d) δ ppm 0.84–0.92 (m, 3 H), 1.25–1.33 (m, 6 H), 1.43–1.53 (m, 2 H), 2.06–2.15 (m, 1 H), 2.89 (dd, J = 13.00, 3.58 Hz, 1 H), 3.05 (dd, J = 12.62, 3.58 Hz, 1 H), 3.16–3.24 (m, 2 H), 3.60–3.69 (m, 1 H), 3.60–3.68 (m, 1 H), 3.83 (dd, J = 13.00, 2.83 Hz, 1 H), 4.01 (ddd, J = 13.38, 3.58, 1.13 Hz, 1 H), 4.41 (dd, J = 11.30, 3.77 Hz, 1 H), 4.59 (s, 1 H), 7.26–7.42 (m, 8 H), 7.47–7.55 (m, 2 H). ESI HRMS m/z: calcd for $C_{25}H_{31}N_3O_3$ 421.24, found 444.22 (M + Na)$^+$.

N-(2-(Methylamino)ethyl)-3-oxo-1,1-diphenyltetrahydro-1H-oxazolo[3,4-a]pyrazine-7(3H)-carboxamide (22). Compound **40** (50 mg, 0.14 mmol) was dissolved in THF (15 mL) and methylamine (2 M soln. in THF, 0.70 mL, 1.4 mmol), and NaHCO$_3$ (29 mg, 0.35 mmol), and KI (13 mg, 0.06 mmol) were added. The reaction mixture was heated to 73 °C for 60 h and concentrated to dryness. The residue was purified using medium pressure column chromatography (12 g of SiO$_2$, 100% ethyl acetate to 50% chloroform/methanol/ammonium hydroxide 80/20/1) to provide **22** (15 mg, 30%). ^{1}H NMR (300 MHz, chloroform-d) δ ppm 1.87 (br s, 1 H), 2.14 (dd, J = 13.19, 11.30 Hz, 1 H), 2.41 (s, 3 H), 2.73 (t, J = 5.65 Hz, 2 H), 2.86 (td, J = 12.81,

3.77 Hz, 1 H), 3.08 (td, J = 12.72, 3.58 Hz, 1 H), 3.23−3.38 (m, 2 H), 3.67−3.75 (m, 1 H), 3.84 (dd, J = 13.19, 2.64 Hz, 1 H), 4.02 (ddd, J = 13.37, 3.58, 1.13 Hz, 1 H), 4.41 (dd, J = 11.30, 3.77 Hz, 1 H), 5.26−5.34 (m, 1 H), 7.25−7.42 (m, 8 H), 7.48−7.58 (m, 2 H). ESI HRMS m/z: calcd for $C_{22}H_{26}N_4O_3$ 394.20, found 395.21 (M + H)$^+$.

N-(3-(Methylamino)propyl)-3-oxo-1,1-diphenyltetrahydro-1H-oxazolo[3,4-a]pyrazine-7(3H)-carboxamide (23). An analogous procedure to that described for **22** using **41** as the starting material provided **23** as a viscous oil (8 mg, 20%). ^{1}H NMR (300 MHz, chloroform-d) δ ppm 1.62−1.67 (m, 3 H), 2.15 (dd, J = 13.37, 11.11 Hz, 1 H), 2.37 (s, 3 H), 2.70−2.78 (m, 2 H), 2.84 (dd, J = 13.19, 3.39 Hz, 1 H), 3.07 (td, J = 12.62, 3.77 Hz, 1 H), 3.28−3.41 (m, 2 H), 3.67−3.77 (m, 1 H), 3.83 (dd, J = 13.37, 2.83 Hz, 1 H), 3.90−3.98 (m, 1 H), 4.41 (dd, J = 11.30, 3.77 Hz, 1 H), 6.92 (d, J = 4.90 Hz, 1 H), 7.26−7.44 (m, 8 H), 7.48−7.56 (m, 2 H). ESI HRMS m/z: calcd for $C_{23}H_{28}N_4O_3$ 408.22, found 409.22 (M + H)$^+$.

N-(3-(Dimethylamino)propyl)-3-oxo-1,1-diphenyltetrahydro-1H-oxazolo[3,4-a]pyrazine-7(3H)-carboxamide (24). An analogous procedure to that described for **22** using **41** and dimethylamine as starting materials provided **24** as a viscous oil (19 mg, 37%). ^{1}H NMR (300 MHz, chloroform-d) δ ppm 1.61−1.68 (m, 3 H), 2.14−2.21 (m, 6 H), 2.37−2.45 (m, 2 H), 2.79−2.87 (m, 1 H), 3.00−3.08 (m, 1 H), 3.28−3.36 (m, 2 H), 3.62−3.73 (m, 1 H), 3.83 (dd, J = 12.81, 2.64 Hz, 1 H), 3.89 (br s, 1 H), 4.40 (dd, J = 11.11, 3.58 Hz, 1 H), 7.16 (br s, 1 H), 7.28−7.44 (m, 8 H), 7.48−7.55 (m, 2 H). ESI HRMS m/z: calcd for $C_{24}H_{30}N_4O_3$ 422.23, found 445.22 (M + Na)$^+$.

1,1-Diphenyl-7-(3-(piperidin-1-yl)propanoyl)tetrahydro-1H-oxazolo[3,4-α]pyrazin-3(5H)-one Trifluoroacetate (25). To a stirred solution of 3-(piperidin-1-yl)propanoic acid was added a 2-fold excess of thionyl chloride, and the reaction mixture was stirred at room temperature for 12 h. The reaction mixture was concentrated to dryness and redissolved in anhydrous CH_2Cl_2 (10 mL, 0.04 mM). To this solution was added **37** (29 mg, 0.1 mmol) and TEA (56 μL, 0.4 mmol). The mixture was allowed to stir at rt for 6 h and was concentrated to dryness. The residue was purified by column chromatography (12 g of SiO_2, 100% methylene chloride to 50% chloroform/methanol/ammonium hydroxide 80/20/1) and then semipreparative HPLC (Synergy Hydro; 15 mL/min 5%−50% B over 30 min) to afford **25** as viscous oil (20 mg, 37%). ^{1}H NMR (300 MHz, chloroform-d) δ ppm 1.32−1.53 (m, 1 H), 2.04 (t, J = 13.00 Hz, 2 H), 2.48−2.96 (m, 5 H), 2.96−3.19 (m, 3 H), 3.19−3.81 (m, 7 H), 3.92 (d, J = 10.17 Hz, 1 H), 4.37 (t, J = 7.72 Hz, 1 H), 4.48−4.69 (m, 1 H), 7.17−7.70 (m, 10 H), 8.77 (br s, 1 H). ESI MS m/z: calcd for $C_{26}H_{31}N_3O_3$ 433.55, found 434 (M + H)$^+$. HPLC (Synergy Hydro, 20 min) t_R = 15.52 min (>99%).

N-(1-Methylpiperidin-4-yl)-3-oxo-1,1-diphenyltetrahydro-1H-oxazolo[3,4-α]pyrazine-7(3H)-carboxamide trifluoroacetate (26). An analogous procedure to that described for **2** using 1-methylpiperidin-4-amine provided crude **26**, which was purified by semipreparative HPLC (Synergy Hydro; 15 mL/min 5%−60% B over 30 min) to afford **26** (25 mg, 26%). ^{1}H NMR (300 MHz, chloroform-d) δ ppm 1.97−2.20 (m, 5 H), 2.75−2.92 (m, 6 H), 3.05 (td, J = 12.62, 3.39 Hz, 1 H), 3.58 (d, J = 12.06 Hz, 2 H), 3.76−4.05 (m, 4 H), 4.38 (dd, J = 11.11, 3.58 Hz, 1 H), 6.52 (br s, 1 H), 7.20−7.44 (m, 8 H), 7.46−7.58 (m, 2 H), 11.56 (br s, 1 H). ESI MS m/z: calcd for $C_{25}H_{30}N_4O_3$ 434.54, found 435.2 (M + H)$^+$, 547.7 (M + TFA − H)$^−$. HPLC (Synergy Hydro, 20 min) t_R = 14.47 min (>99%).

tert-Butyl-1-(3-oxo-1,1-diphenylhexahydro-1H-oxazolo[3,4-α]-pyrazine-7-carbonyl)pyrrolidin-3-ylcarbamate (27). An analogous procedure to that described for **2** using *tert*-butyl pyrrolidin-3-ylcarbamate provided **27** as a viscous oil (37 mg, 43%). ^{1}H NMR (300 MHz, chloroform-d) δ ppm 1.42−1.48 (m, 9 H), 1.60−1.92 (m, 1 H), 2.02−2.24 (m, 2 H), 2.87 (br s, 1 H), 3.02−3.25 (m, 2 H), 3.34−3.66 (m, 6 H), 3.71−3.90 (m, 2 H), 4.09−4.21 (m, 1 H), 4.55 (ddd, J = 10.83, 6.88, 3.39 Hz, 1 H), 7.28−7.44 (m, 8 H), 7.50−7.57 (m, 2 H). ESI MS m/z: calcd for $C_{28}H_{34}N_4O_5$ 506.60, found 507.1 (M + H)$^+$, 505.6 (M − H)$^−$. HPLC (Synergy Hydro, 20 min) t_R = 19.45 min (80%).

7-(3-Aminopyrrolidine-1-carbonyl)-1,1-diphenyltetrahydro-1H-oxazolo[3,4-α]pyrazin-3(5H)-one Trifluoroacetate (28). To a solution of **27** (35 mg, 0.7 mmol) in CH_2Cl_2 (3 mL) was added trifluoroacetic acid (0.3 mL). The reaction mixture was allowed to stir at rt for 3 h and was concentrated to dryness. Purification by semipreparative HPLC (Synergy Hydro; 15 mL/min 5%−60% B over 30 min) provided **28** as a white solid (28 mg, 77%). ^{1}H NMR (300 MHz, DMSO-d_6) δ ppm 1.82−1.95 (m, 1 H), 2.06−2.20 (m, 2 H), 2.65−2.78 (m, 1 H), 3.05−3.21 (m, 1 H), 3.27 (dt, J = 11.59, 4.00 Hz, 1 H), 3.33−3.70 (m, 6 H), 3.75 (d, J = 4.52 Hz, 1 H), 4.64 (ddd, J = 10.83, 6.31, 3.58 Hz, 1 H), 7.29−7.48 (m, 8 H), 7.58 (d, J = 7.54 Hz, 2 H), 8.12 (br s, 3 H). ESI MS m/z: calcd for $C_{28}H_{34}N_4O_5$ 406.49, found 407.6 (M + H)$^+$. HPLC (Synergy Hydro, 20 min) t_R = 13.89 min (>99%).

(3S)-tert-Butyl-3-(3-oxo-1,1-diphenylhexahydro-1H-oxazolo[3,4-α]pyrazine-7-carboxamido)pyrrolidine-1-carboxylate (29). An analogous procedure to that described for **2** using (S)-*tert*-butyl 3-aminopyrrolidine-1-carboxylate provided **29** as a viscous oil (46 mg, 53%). ^{1}H NMR (300 MHz, chloroform-d) δ ppm 1.39−1.52 (m, 9 H), 2.08−2.23 (m, 2 H), 2.85−3.01 (m, 1 H), 3.02−3.16 (m, 2 H), 3.41 (br s, 2 H), 3.61 (d, J = 5.65 Hz, 2 H), 3.84 (br s, 1 H), 3.94−4.07 (m, 1 H), 4.27−4.38 (m, 1 H), 4.38−4.49 (m, 2 H), 7.27−7.46 (m, 8 H), 7.47−7.57 (m, 2 H). ESI MS m/z: calcd for $C_{28}H_{34}N_4O_5$ 506.60, found 407.4 ($C_{28}H_{34}N_4O_5$ − Boc + H)$^+$, 507.2 ($C_{28}H_{34}N_4O_5$ + H)$^+$. HPLC (Synergy Hydro, 20 min) t_R = 19.48 min (83.4%).

3-Oxo-1,1-diphenyl-N-((S)-pyrrolidin-3-yl)tetrahydro-1H-oxazolo[3,4-α]pyrazine-7(3H)-carboxamide Trifluoroacetate (30). An analogous procedure to that described for **28** provided **30** (35 mg, 75%). ^{1}H NMR (300 MHz, chloroform-d) δ ppm 2.05−2.21 (m, 2 H), 2.35 (d, J = 7.16 Hz, 1 H), 2.71−2.92 (m, 1 H), 3.03 (t, J = 12.24 Hz, 1 H), 3.17−3.62 (m, 4 H), 3.84 (t, J = 13.00 Hz, 2 H), 3.95−4.12 (m, 1 H), 4.40 (ddd, J = 11.02, 7.44, 3.77 Hz, 1 H), 4.60 (br s, 1 H), 7.28−7.43 (m, 8 H), 7.45−7.58 (m, 2 H), 8.78 (br s, 1 H), 9.84 (br s, 1 H). ESI MS m/z: calcd for $C_{28}H_{34}N_4O_5$ 406.49, found 407.4 (M + H)$^+$, 519.5 (M + TFA − H)$^−$. HPLC (Synergy Hydro, 20 min) t_R = 13.97 min (>99%).

(−3aS)-N-(4-Fluorobenzyl)-3-oxo-1,1-diphenyltetrahydro-1H-oxazolo[3,4-a]pyrazine-7(3H)-carboxamide (31). An analogous procedure to that described for **1** using **38** provided **31** as a colorless semisolid (8.0 mg, 30%). ^{1}H NMR (300 MHz, chloroform-d) δ ppm 2.17 (dd, J = 13.19, 11.30 Hz, 1 H), 2.83−3.00 (m, 1 H), 3.01−3.16 (m, 1 H), 3.63 (dd, J = 13.00, 1.70 Hz, 1 H), 3.86 (dd, J = 13.00, 2.45 Hz, 1 H), 4.03 (dd, J = 13.19, 2.26 Hz, 1 H), 4.26−4.49 (m, 3 H), 4.69−4.81 (m, 1 H), 6.95−7.09 (m, 1 H), 7.21−7.45 (m, 11 H), 7.47−7.56 (m, 2 H). t_R = 11.47 min, peak 1, Chiralpak-IA 4.6 mm × 250 mm column, in 9:1 hexane/isopropanol at a flow rate of 1 mL/min. ESI MS m/z: calcd for $C_{26}H_{24}FN_3O_3$ 445.49, found 446.7 (M + H)$^+$. $[\alpha]_D^{20}$ = −151 (c = 0.585, CHCl$_3$).

(+3aR)-N-(4-Fluorobenzyl)-3-oxo-1,1-diphenyltetrahydro-1H-oxazolo[3,4-a]pyrazine-7(3H)-carboxamide (32). An analogous procedure to that described for **1** using **39** provided **32** as a colorless semisolid (8 mg, 30%). ^{1}H NMR (300 MHz, chloroform-d) δ ppm 2.17 (dd, J = 13.19, 11.30 Hz, 1 H), 2.83−3.00 (m, 1 H), 3.01−3.16 (m, 1 H), 3.63 (dd, J = 13.00, 1.70 Hz, 1 H), 3.86 (dd, J = 13.00, 2.45 Hz, 1 H), 4.03 (dd, J = 13.19, 2.26 Hz, 1 H), 4.26−4.49 (m, 3 H), 4.69−4.81 (m, 1 H), 6.95−7.09 (m, 1 H), 7.21−7.45 (m, 11 H), 7.47−7.56 (m, 2 H); t_R = 14.77 min, peak 2, Chiralpak-IA 4.6 mm × 250 mm column, in 9:1 hexane/isopropanol at a flow rate of 1 mL/min. ESI MS m/z: calcd for $C_{26}H_{24}FN_3O_3$ 445.49, found 446.7 (M + H)$^+$.

(−3aS)-3-Oxo-1,1-diphenyl-N-(2-(piperidin-1-yl)ethyl)tetrahydro-1H-oxazolo[3,4-a]pyrazine-7(3H)-carboxamide (33). Compound **33** was isolated from racemic **2** via semipreparative chiral chromatography on a Chiralpak-IA 20 mm × 250 mm column, utilizing an isocratic method (95:5:0.1 hexane/isopropanol/diethyl amine) at a flow rate of 12 mL/min (100 mg in 400 μL of ethanol/DMSO), to obtain 7.3 mg (t_R = 10.45 min, peak 1). $[\alpha]_D^{20}$ = −142 (c = 0.81, methanol).

(+3aR)-3-Oxo-1,1-diphenyl-N-(2-(piperidin-1-yl)ethyl)tetrahydro-1H-oxazolo[3,4-a]pyrazine-7(3H)-carboxamide (34). Fractions from the isolation of compound **33** that were enriched in compound **34** were pooled (49 mg, 95% enantiomeric purity) and rechromato-graphed utilizing the same column and isocratic method (40 mg in 400

μL of ethanol/DMSO) to obtain 26.2 mg of pure **34** as a colorless oil (t_R = 12.67 min, peak 2); $[\alpha]^D_{20}$ = +138 (c = 0.82, methanol).

(1,4-Dibenzylpiperazin-2-yl)diphenylmethanol (35). To a solution of phenyl lithium (74.7 mL, 1.8 M in dibutylether) and THF (anhydrous, 170 mL) at −78 °C was added dropwise a solution of ethyl 1,4-dibenzylpiperazine-2-carboxylate (9 g, 26.59 mmol) in THF (anhydrous, 100 mL). After complete addition, the reaction mixture was warmed to room temperature over 30 min and then stirred at rt for 1 h. The reaction mixture was quenched with H_2O (200 mL) and extracted with CH_2Cl_2 (2 × 250 mL). The organic layer was dried ($MgSO_4$), concentrated, and purified by medium pressure column chromatography (80 g of SiO_2, 100% CH_2Cl_2) to provide **35** as a yellow solid (11.92 g, quant.). ^{1}H NMR (300 MHz, chloroform-*d*) δ ppm 1.56 (br s, 1 H), 2.32−2.48 (m, 2 H), 2.48−2.61 (m, 2 H), 2.79 (d, J = 11.68 Hz, 1 H), 3.28−3.46 (m, 2 H), 3.53−3.78 (m, 4 H), 6.96−7.35 (m, 16 H), 7.35−7.45 (m, 2 H), 7.45−7.54 (m, 2 H). ESI MS m/z: calcd for $C_{31}H_{32}N_2O$ 448.6, found 449.7 (M + H)$^+$, 448.0 (M − H)$^-$.

Diphenyl(piperazin-2-yl)methanol (36). To a solution of **35** (2.54 g, 5.76 mmol) in CH_2Cl_2 (100 mL) was added 1 N HCl in Et_2O (8.5 mL, 8.5 mmol). The reaction mixture was allowed to stir at room temperature for 1 h and concentrated to dryness, and the residual white powder was dried under high vacuum for 1 h. The residue was redissolved in hot ethanol (110 mL) and hydrogenated (46 psi) over 5% Pd/BaSO$_4$ (1 g) and 10% Pd/C (1 g) at rt for 20 h. The reaction mixture was filtered through Celite, and the filtrate was concentrated to dryness. The resulting residue was suspended in CH_2Cl_2 (200 mL) and washed with aq. NaOH (1 N, 50 mL). The aqueous layer was extracted with CH_2Cl_2 (2 × 200 mL); the combined organic layers were washed with brine (2 × 50 mL), dried ($MgSO_4$), and concentrated to dryness to provide crude **36** (1.16 g) as a yellow solid. ^{1}H NMR (300 MHz, chloroform-*d*) δ ppm 1.60 (br s, 2 H), 2.56−2.77 (m, 3 H), 2.83−3.05 (m, 3 H), 3.70 (dd, J = 9.42, 3.39 Hz, 1 H), 4.48 (br s, 1 H), 7.11−7.38 (m, 6 H), 7.49 (dd, J = 8.29, 1.13 Hz, 2 H), 7.57−7.67 (m, 2 H). ESI MS m/z: calcd for $C_{17}H_{20}N_2O$ 268.36, found 269.4 (M + H)$^+$, 251.2 (M − HO)$^+$. HPLC t_R = 10.57 min (>99%).

1,1-Diphenyltetrahydro-1H-oxazolo[3,4-α]pyrazin-3(5H)-one (37). To a solution of **36** (1g, 3.73 mmol) in THF (anhydrous, 100 mL) was added di-*t*-butyl dicarbonate (2.03 g, 9.32 mmol), NEt$_3$ (1.3 mL, 9.32 mmol), and DMAP (1.13 g, 9.32 mmol). The reaction mixture was allowed to stir at rt for 2 h, concentrated to dryness, and redissolved in CH_2Cl_2 (100 mL). The solution was washed with aq. sat. NaHCO$_3$ (50 mL) and brine (50 mL), dried ($MgSO_4$), and concentrated. The resulting semisolid was redissolved in CH_2Cl_2 (200 mL), and TFA (2.85 mL, 37.3 mmol) was added. The reaction mixture was stirred at room temperature for 8 h, concentrated to dryness, and redissolved in CH_2Cl_2 (100 mL). The solution was washed with aq. sat. NaHCO$_3$ (2 × 50 mL), dried ($MgSO_4$), and concentrated. The residue was purified by column chromatography (80 g of SiO_2, 100% methylene chloride to 40% chloroform/methanol/ammonium hydroxide 80/20/1) to provide **37** as a white solid (900 mg, 82% over three steps). ^{1}H NMR (300 MHz, DMSO-*d*$_6$) δ ppm 2.38−2.48 (m, 1 H), 2.89−3.09 (m, 1 H), 3.09−3.21 (m, 1 H), 3.21−3.43 (m, 2 H), 3.82 (dd, J = 14.13, 3.96 Hz, 1 H), 4.91 (dd, J = 11.68, 3.39 Hz, 1 H), 7.25−7.61 (m, 10 H), 9.33 (br s, 1 H). ESI MS m/z: calcd for $C_{18}H_{18}N_2O_2$ 294.35, found 295.2 (M + H)$^+$. HPLC (Synergy Hydro, 20 min) t_R = 13.59 min (95.1%).

(−3aS)-1,1-Diphenyltetrahydro-1H-oxazolo[3,4-α]pyrazin-3(5H)-one (38). Compound **38** was isolated from racemic **37** via semipreparative chiral chromatography on a Chiralpak-IA 20 mm × 250 mm column, utilizing an isocratic method (95:5:0.1 hexane/isopropanol/diethyl amine) at a flow rate of 12 mL/min over 13 identical separations (40 mg in 150 μL of ethanol/DMSO per run), to obtain 104.8 mg as a colorless oil (t_R = 17.2 min, peak 1); $[\alpha]^{20}_D$ = −258.5 (c = 0.265, MeOH).

(−3aS)-1,1-Diphenyltetrahydro-1H-oxazolo[3,4-α]pyrazin-3(5H)-one R-Camphor Sulfonate (38a). Compound **38** (0.088 g, 0.30 mmol) was dissolved in MeOH (15 mL) and (R)-camphor sulfonic acid (0.069 g, 0.30 mmol) was added. The suspension was warmed

until the solid dissolved and was allowed to stand at room temperature for 8 h. The resulting crystals were collected and dried under reduced pressure to afford **38a** as colorless needles (0.106 g), mp =211−213 °C; $[\alpha]^{20}_D$ = −151.43 (c = 0.175, MeOH). Compound **38a** was sent for X-ray analysis.

(+3aR)-1,1-Diphenyltetrahydro-1H-oxazolo[3,4-α]pyrazin-3(5H)-one (39). Fractions from the isolation of compound **38** that were enriched in compound **39** were pooled (126 mg, 93% enantiomeric purity) and rechromatographed over six separations (16 mg in 100 μL of ethanol/DMSO per run) utilizing the same column and isocratic method to obtain 85.7 mg of pure **39** as a colorless oil (t_R = 23.4 min, peak 2). $[\alpha]^{20}_D$ = +252.8 (c = 0.345, MeOH).

N-(2-Chloroethyl)-3-oxo-1,1-diphenyltetrahydro-1H-oxazolo[3,4-a]pyrazine-7(3H)-carboxamide (40). An analogous procedure to that described for **1** using 2-chloroethyl isocyanate provided **40** as a viscous oil (39 mg, 61%). ^{1}H NMR (300 MHz, chloroform-d) δ ppm 2.09−2.26 (m, 1 H), 2.74−2.95 (m, 1 H), 3.08 (td, J = 12.62, 3.77 Hz, 1 H), 3.44−3.68 (m, 4 H), 3.70−3.87 (m, 2 H), 3.98 (dd, J = 13.56, 2.26 Hz, 1 H), 4.42 (dd, J = 11.30, 3.77 Hz, 1 H), 5.33 (t, J = 5.09 Hz, 1 H), 7.18−7.43 (m, 8 H), 7.44−7.60 (m, 2 H).

N-(3-Chloropropyl)-3-oxo-1,1-diphenyltetrahydro-1H-oxazolo-[3,4-a]pyrazine-7(3H)-carboxamide (41). An analogous procedure to that described for **1** using 3-chloropropylisocyanate provided **41** as a viscous oil (195 mg, %). ^{1}H NMR (300 MHz, chloroform-*d*) δ ppm 1.92−2.02 (m, 2 H), 2.14 (dd, J = 13.56, 11.30 Hz, 1 H), 2.77−2.94 (m, 1 H), 3.06 (td, J = 12.62, 3.77 Hz, 1 H), 3.38 (qd, J = 6.22, 2.83 Hz, 2 H), 3.52−3.64 (m, 2 H), 3.64−3.76 (m, 1 H), 3.83 (dd, J = 13.19, 2.64 Hz, 1 H), 3.97 (ddd, J = 13.37, 3.58, 1.13 Hz, 1 H), 4.41 (dd, J = 11.11, 3.58 Hz, 1 H), 5.00 (t, J = 5.65 Hz, 1 H), 7.24−7.43 (m, 8 H), 7.46−7.55 (m, 2 H).

X-ray Crystallographic Analysis. Single-crystal X-ray diffraction data on compound **38a** was collected using Cu Kα radiation and a Bruker Platinum-135 CCD area detector. The crystal was prepared for data collection by coating with high viscosity microscope oil. The oil-coated crystal was mounted on a micromesh mount (Mitergen, Inc.) and transferred to the diffractometer, and a data set was collected at 150 K. The 0.205 × 0.010 × 0.005 mm^3 crystal was monoclinic in space group P2$_1$, with unit cell dimensions a = 11.5583(6), b = 7.2211(4), c = 16.4478(9) Å and β = 103.333(2)°. Data was 72.7% complete to 66.79°θ (~0.83 Å) with an average redundancy of 1.67. The structure was solved by direct methods and refined by full-matrix least-squares on F^2 values using the programs found in the SHELXTL suite (Bruker, SHELXTL v6.10, 2000, Bruker AXS Inc., Madison, WI). Corrections were applied for Lorentz, polarization, and absorption effects. Parameters refined included atomic coordinates and aniso-tropic thermal parameters for all non-hydrogen atoms. Hydrogen atoms on carbons were included using a riding model [coordinate shifts of C applied to H atoms] with C−H distance set at 0.96 Å. The final anisotropic full matrix least-squares refinement on F^2 with 336 variables and one restraint converged at R1 = 3.85% for the observed data and wR2 = 9.89% for all data. The absolute configuration was determined from the X-ray data using the method of Flack.[35] Complete information on data collection and refinement is available in the Supporting Information.

Atomic coordinates for **38a** have been deposited with the Cambridge Crystallographic Data Centre (deposition number 978117). Copies of the data can be obtained, free of charge, on application to CCDC, 12 Union Road, Cambridge, CB2 1EZ, UK [fax: +44(0)-1223-336033 or e-mail: deposit@ccdc.cam.ac.uk.

In Vitro Functional Assays. Functional determinations, identification of functional antagonists at the NPSR, utilized RD-HGA16 cells (Molecular Devices), a CHO cell line stably overexpressing the promiscuous Gq-protein Ga16. Two individual cell lines were created that stably express each NPSR variant (NPS Ile107 and Asn107). Cells were loaded with the calcium sensitive dye calcium3 (Molecular Devices) for 1 h, and compounds were assayed in separate experiments for intrinsic activity and for the ability to inhibit NPS activity as measured by calcium mobilization in the FlexStation assay. All test compounds were evaluated for activity at least three times, and each experiment was conducted on a different day. Apparent constant

K_e is determined by running the EC_{50} curves of the agonist, NPS, with and without the test compounds and measuring the rightward shift of the agonist curve. K_e values were calculated using the equation $K_e = [L]/((EC_{50}^-/EC_{50}^+) - 1)$ where $[L]$ is the test compound concentration, EC_{50}^- is the EC_{50} of NPS alone, and EC_{50}^+ is the EC_{50} of NPS in the presence of test compound. Therefore, the K_e value is independent of the concentration of test compounds. A three-parameter logistic equation was fit to the concentration response data with Prism (v5 for Windows, GraphPad Software; San Diego, CA) to calculate the EC_{50} and K_e values. NPS EC_{50} values for all experiments were in the range of 0.25−1.13 nM at the 107I and 5.1−11.2 nM for the 107N variant.

NPS Induced Locomotion. Male C57Bl/6 mice (National Cancer Institute, Bethesda, MD), age 8−12 weeks, were group housed (four animals per cage) under controlled conditions (temperature 21 ± 2 °C; relative humidity 50%−60%; 12 h light−dark cycle, lights on 6:00 AM) with free access to food and water. Prior to drug injections, mice were briefly anesthetized with halothane.

Locomotion of mice was monitored in rectangular plexiglass boxes (60 cm × 40 cm × 50 cm) and cumulative distance traveled (total distance in centimeters that the animal traveled during the test) was measured with an automated activity monitor system (Versamax, Accuscan, Columbus, OH). Mice were allowed to habituate to the recording chamber for 60 min. Vehicle or compound **34** (in PBS, 10% Cremophor EL) were injected ip 10 min before the central administration of either NPS (1 nmol in 2 μL of PBS, 0.1% BSA) or vehicle (PBS, 0.1% BSA), as describe in Xu et al.[2] Mice were allowed to recover for 5 min and then placed into the apparatus. Recording of locomotor activity continued for 90 min.

Pharmacokinetic Analysis. Male C57Bl/6 mice were purchased from Charles River Laboratories (Raleigh, NC) at a target weight of 25−30 g corresponding to ages of approximately 8 weeks at receipt. Mice were dosed at 5 mg/kg with a single dose of **34** as a solution in 2.5% dimethylacetamide, 2.5% Cremophor EL, and 95% phosphate buffered saline, at a final concentration of 0.5 mg/mL. Blood samples were collected via cardiac puncture from five mice per time point at target time points of 15 min, 30 min, 1 h, and 2 h postdose. At sacrifice, the brain of each animal was removed, weighed, and immediately flash-frozen using liquid nitrogen within low density polyethylene vials. Whole brain samples were homogenized using a Potter−Elvehjem type homogenizer in ethanol/water (50:50, v/v) solution, which was added in a ratio of 3 mL per gram of brain. A 50 μL aliquot of brain homogenate or plasma was transferred to microcentrifuge tubes followed by 200 μL of deionized/distilled water and 1.2 mL of a 10 ng/mL solution of reserpine internal standard in acetonitrile. The samples were vortexed and centrifuged in a model 5415C microcentrifuge (Eppendorf North America, Westbury NY) at 16000g and transferred to autosampler vials for analysis. Calibration standards were prepared by combining 40 μL blank plasma or blank brain homogenate and 10 μL of **34** spiking solution in microcentrifuge tubes and 1.2 mL internal standard solution in acetonitrile. Sample analysis was conducted using an Applied Biosystems API 5000 triple quadrupole mass spectrometer (Foster City Ca) interfaced to Agilent 1100 binary pump and autosampler. A Valco valve and Agilent 1100 isocratic pump were used to divert the first minute of the run to waste while infusing 50:50 acetonitrile/water makeup solvent to the mass spectrometer. Chromatography was accomplished using a Phenomenex Luna C18 column (50 mm × 2 mm i.d., 5 μm particle size) fitted with a guard cartridge. Injection volumes were 10 μL. Two mobile phase solutions were used: solution A was 0.1% formic acid in water, and solution B was 0.1% formic acid in methanol, and the flow rate was 0.5 mL/min. Initial chromatographic conditions were 90% A then decreasing to 5% A over 4 min, then returning to initial conditions for 2 min for column equilibration. Compound **34** was monitored in positive electrospray mode with an MRM transition of 449.20 → 155.10 with DP = 50, CE = 39, and CXP = 36. Reserpine internals standard was monitored with a transition of 609.20 → 195.00 with DP = 231, CE = 41, and CXP = 14. Mass spectrometer parameters were as follows: CUR = 13, GS1 = 50, GS2 = 50, IS = 4000, TEM = 600 °C, and CAD = 8.

Pharmacokinetic analyses were conducted using WinNonlin (version 5.2; Pharsight Corporation, Mountainview CA). Mean plasma concentration vs time data for **34** was analyzed using noncompartmental methods (models 200, WinNonlin) to determine pharmacokinetic parameter estimates. The following parameters were estimated: maximum observed plasma concentration and time at which the maximum concentration was observed (C_{max} and T_{max}, respectively); terminal elimination rate constant (λ_z) and terminal half-life ($t_{1/2}$); area under the plasma concentration vs time curve (AUC) to last time point with measurable **34** concentration (AUC_{last}) and AUC extrapolated to infinity (AUC_{0-inf}). The concentration−time data of **34** in the brain were also analyzed similarly. Given the limited amount of data collected in this study, statistical analyses were not conducted.

■ ASSOCIATED CONTENT

⑤ Supporting Information

HPLC analysis and MS of target compounds. This material is available free of charge via the Internet at http://pubs.acs.org.

■ AUTHOR INFORMATION

Corresponding Author
*Scott P. Runyon. E-mail: srunyon@rti.org. Telephone: 919 316-3842. Fax: 919 541-8868.

Author Contributions

The manuscript was written through contributions of all authors. All authors have given approval to the final version of the manuscript.

Notes

The authors declare no competing financial interest.

■ ACKNOWLEDGMENTS

■ ABBREVIATIONS

ANOVA Analysis of variance; API atmospheric pressure ionization; cAMP cyclic adenosine monophosphate; CNS central nervous system; CRF corticotrophin releasing factor; CSA camphor sulfonic acid; DEA diethylamine; DMSO dimethyl sulfoxide; GPCR G-protein coupled receptor; HTS high throughput screen; LC/MS liquid chromatography−mass spectrometry; LC locus ceruleus; NPS neuropeptide S; NPSR neuropeptide S receptor; PTSD posttraumatic stress disorder; TFA trifluoroacetic acid; TLC thin-layer chromatography; VTA ventral tegmental area

■ REFERENCES

(1) Sato, S. Shintani, Y.; Miyajima, N.; Yoshimura, K., Novel G-protein coupled receptor protein and DNA thereof. World Patent Application WO 2002031145 A1, 2002.

(2) Xu, Y. L., Reinscheid, R. K., Huitron-Resendiz, S., Clark, S. D., Wang, Z., Lin, S. H., Brucher, F. A., Zeng, J., Ly, N. K., Henriksen, S. J., de Lecea, L., Civelli, O., and Neuropeptide, S. (2004) A neuropeptide promoting arousal and anxiolytic-like effects. *Neuron 43* (4), 487−497.

(3) Xu, Y. L., Gall, C. M., Jackson, V. R., Civelli, O., and Reinscheid, R. K. (2007) Distribution of neuropeptide S receptor mRNA and

neurochemical characteristics of neuropeptide S-expressing neurons in the rat brain. *J. Comp. Neurol.* 500 (1), 84−102.

(4) Clark, S. D., Duangdao, D. M., Schulz, S., Zhang, L., Liu, X., Xu, Y. L., and Reinscheid, R. K. (2011) Anatomical characterization of the neuropeptide S system in the mouse brain by in situ hybridization and immunohistochemistry. *J. Comp. Neurol.* 519 (10), 1867−1893.

(5) Reinscheid, R. K., and Xu, Y. L. (2005) Neuropeptide S and its receptor: A newly deorphanized G protein-coupled receptor system. *Neuroscientist 11* (6), 532−538.

(6) Domschke, K., Reif, A., Weber, H., Richter, J., Hohoff, C., Ohrmann, P., Pedersen, A., Bauer, J., Suslow, T., Kugel, H., Heindel, W., Baumann, C., Klauke, B., Jacob, C., Maier, W., Fritze, J., Bandelow, B., Krakowitzky, P., Rothermundt, M., Erhardt, A., Binder, E. B., Holsboer, F., Gerlach, A. L., Kircher, T., Lang, T., Alpers, G. W., Strohle, A., Fehm, L., Gloster, A. T., Wittchen, H. U., Arolt, V., Pauli, P., Hamm, A., and Deckert, J. (2010) Neuropeptide S receptor gene — converging evidence for a role in panic disorder. *Mol. Psychiatry 16*, 938−948.

(7) Okamura, N., Hashimoto, K., Iyo, M., Shimizu, E., Dempfle, A., Friedel, S., and Reinscheid, R. K. (2007) Gender-specific association of a functional coding polymorphism in the Neuropeptide S receptor gene with panic disorder but not with schizophrenia or attention-deficit/hyperactivity disorder. *Prog. Neuropsychopharmacol. Biol. Psychiatry 31* (7), 1444−1448.

(8) Raczka, K. A., Gartmann, N., Mechias, M. L., Reif, A., Buchel, C., Deckert, J., and Kalisch, R. (2010) A neuropeptide S receptor variant associated with overinterpretation of fear reactions: a potential neurogenetic basis for catastrophizing. *Mol. Psychiatry 15*, 1067−1074.

(9) Leonard, S. K., Dwyer, J. M., Sukoff Rizzo, S. J., Platt, B., Logue, S. F., Neal, S. J., Malberg, J. E., Beyer, C. E., Schechter, L. E., Rosenzweig-Lipson, S., and Ring, R. H. (2008) Pharmacology of neuropeptide S in mice: therapeutic relevance to anxiety disorders. *Psychopharmacology (Berlin) 197* (4), 601−611.

(10) Rizzi, A., Vergura, R., Marzola, G., Ruzza, C., Guerrini, R., Salvadori, S., Regoli, D., and Calo, G. (2008) Neuropeptide S is a stimulatory anxiolytic agent: a behavioural study in mice. *Br. J. Pharmacol. 154*, 471−479.

(11) Vitale, G., Filaferro, M., Ruggieri, V., Pennella, S., Frigeri, C., Rizzi, A., Guerrini, R., and Calo, G. (2008) Anxiolytic-like effect of neuropeptide S in the rat defensive burying. *Peptides 29* (12), 2286−2291.

(12) Gottlieb, D. J., O'Connor, G. T., and Wilk, J. B. (2007) Genome-wide association of sleep and circadian phenotypes. *BMC Med. Genet. 8* (Suppl 1), No. S9.

(13) Laitinen, T., Polvi, A., Rydman, P., Vendelin, J., Pulkkinen, V., Salmikangas, P., Makela, S., Rehn, M., Pirskanen, A., Rautanen, A., Zucchelli, M., Gullsten, H., Leino, M., Alenius, H., Petays, T., Haahtela, T., Laitinen, A., Laprise, C., Hudson, T. J., Laitinen, L. A., and Kere, J. (2004) Characterization of a common susceptibility locus for asthma-related traits. *Science 304* (5668), 300−304.

(14) Cline, M. A., Godlove, D. C., Nandar, W., Bowden, C. N., and Prall, B. C. (2007) Anorexigenic effects of central neuropeptide S involve the hypothalamus in chicks (*Gallus gallus*). *Comp. Biochem. Physiol., Part A: Mol. Integr. Physiol. 148* (3), 657−663.

(15) Cline, M. A., Prall, B. C., Smith, M. L., Calchary, W. A., and Siegel, P. B. (2008) Differential appetite-related responses to central neuropeptide S in lines of chickens divergently selected for low or high body weight. *J. Neuroendocrinol 20* (7), 904−908.

(16) Meis, S., Bergado-Acosta, J. R., Yanagawa, Y., Obata, K., Stork, O., and Munsch, T. (2008) Identification of a neuropeptide S responsive circuitry shaping amygdala activity via the endopiriform nucleus. *PLoS One 3* (7), No. e2695.

(17) Jungling, K., Seidenbecher, T., Sosulina, L., Lesting, J., Sangha, S., Clark, S. D., Okamura, N., Duangdao, D. M., Xu, Y. L., Reinscheid, R. K., and Pape, H. C. (2008) Neuropeptide S-mediated control of fear expression and extinction: Role of intercalated GABAergic neurons in the amygdala. *Neuron 59* (2), 298−310.

(18) Cioccioppo, R., Economidou, D., Cannella, N., Braconi, S., Stopponi, S. (2007) Neuropeptide s system activation facilitates

conditioned reinstatement of cocaine-seeking in the rat. Presented at the Society for Neuroscience 2007, San Diego, 271.18/Z1.

(19) Badia-Elder, N. E., Henderson, A. N., Bertholomey, M. L., Dodge, N. C., and Stewart, R. B. (2008) The effects of neuropeptide S on ethanol drinking and other related behaviors in alcohol-preferring and -nonpreferring rats. *Alcohol.: Clin. Exp. Res. 32* (8), 1380−1387.

(20) Schmoutz, C. D., Zhang, Y., Runyon, S. P., and Goeders, N. E. (2012) Antagonism of the neuropeptide S receptor with RTI-118 decreases cocaine self-administration and cocaine-seeking behavior in rats. *Pharmacol., Biochem. Behav. 103* (2), 332−337.

(21) Cardenas, A., Gines, P., and Runyon, B. A. (2009) Is albumin infusion necessary after large volume paracentesis? *Liver Int. 29* (5), 636−640, () 640−641 discussion.

(22) Si, W., Aluisio, L., Okamura, N., Clark, S. D., Fraser, I., Sutton, S. W., Bonaventure, P., and Reinscheid, R. K. (2010) Neuropeptide S stimulates dopaminergic neurotransmission in the medial prefrontal cortex. *J. Neurochem 115*, 475−482.

(23) Mochizuki, T., Kim, J., and Sasaki, K. (2010) Microinjection of neuropeptide S into the rat ventral tegmental area induces hyper-activity and increases extracellular levels of dopamine metabolites in the nucleus accumbens shell. *Peptides 31* (5), 926−931.

(24) Paneda, C., Huitron-Resendiz, S., Frago, L. M., Chowen, J. A., Picetti, R., de Lecea, L., and Roberts, A. J. (2009) Neuropeptide S reinstates cocaine-seeking behavior and increases locomotor activity through corticotropin-releasing factor receptor 1 in mice. *J. Neurosci. 29* (13), 4155−4161.

(25) Kallupi, M., Cannella, N., Economidou, D., Ubaldi, M., Ruggeri, B., Weiss, F., Massi, M., Marugan, J., Heilig, M., Bonnavion, P., de Lecea, L., and Ciccocioppo, R. (2010) Neuropeptide S facilitates cue-induced relapse to cocaine seeking through activation of the hypothalamic hypocretin system. *Proc. Natl. Acad. Sci. U. S. A. 107* (45), 19567−19572.

(26) Okamura, N., Habay, S. A., Zeng, J., Chamberlin, A. R., and Reinscheid, R. K. (2008) Synthesis and pharmacological in vitro and in vivo profile of 3-oxo-1,1-diphenyl-tetrahydro-oxazolo[3,4-a]pyrazine-7-carboxylic acid 4-fluoro-benzylamide (SHA 68), a selective antagonist of the neuropeptide S receptor. *J. Pharmacol. Exp. Ther. 325* (3), 893−901.

(27) Zhang, Y., Gilmour, B. P., Navarro, H. A., and Runyon, S. P. (2008) Identifying structural features on 1,1-diphenyl-hexahydro-oxazolo[3,4-a]pyrazin-3-ones critical for Neuropeptide S antagonist activity. *Bioorg. Med. Chem. Lett. 18* (14), 4064−4067.

(28) Melamed, J. Y., Zartman, A. E., Kett, N. R., Gotter, A. L., Uebele, V. N., Reiss, D. R., Condra, C. L., Fandozzi, C., Lubbers, L. S., Rowe, B. A., McGaughey, G. B., Henault, M., Stocco, R., Renger, J. J., Hartman, G. D., Bilodeau, M. T., and Trotter, B. W. (2010) Synthesis and evaluation of a new series of Neuropeptide S receptor antagonists. *Bioorg. Med. Chem. Lett. 20* (15), 4700−4703.

(29) Trotter, B. W., Nanda, K. K., Manley, P. J., Uebele, V. N., Condra, C. L., Gotter, A. L., Menzel, K., Henault, M., Stocco, R., Renger, J. J., Hartman, G. D., and Bilodeau, M. T. (2010) Tricyclic imidazole antagonists of the Neuropeptide S Receptor. *Bioorg. Med. Chem. Lett. 20* (15), 4704−4708.

(30) Micheli, F., Di Fabio, R., Giacometti, A., Roth, A., Moro, E., Merlo, G., Paio, A., Merlo-Pich, E., Tomelleri, S., Tonelli, F., Zarantonello, P., Zonzini, L., and Capelli, A. M. (2010) Synthesis and pharmacological characterization of 5-phenyl-2-[2-(1-piperidinylcarbonyl)phenyl]-2,3-dihydro-1H-pyrrolo[1,2-c]imidazo l-1-ones: a new class of Neuropeptide S antagonists. *Bioorg. Med. Chem. Lett. 20* (24), 7308−7311.

(31) Thorsell, A., Tapocik, J. D., Liu, K., Zook, M., Bell, L., Flanigan, M., Patnaik, S., Marugan, J., Damadzic, R., Dehdashti, S. J., Schwandt, M. L., Southall, N., Austin, C. P., Eskay, R., Ciccocioppo, R., Zheng, W., and Heilig, M. (2013) A novel brain penetrant NPS receptor antagonist, NCGC00185684, blocks alcohol-induced ERK-phosphory-lation in the central amygdala and decreases operant alcohol self-administration in rats. *J. Neurosci. 33* (24), 10132−10142.

(32) Knölker, H. J., and Braxmeier, T. (1998) Isocyanates. Part 5. Synthesis of chiral oxazolidin-2-ones and imidazolidin-2-ones via

DMAP-catalyzed isocyanation of amines with di-tert-butyl dicarbonate. *Tetrahedron Lett.* 39 (51), 9407−9410.

(33) Roy, D., Ducher, F., Laumain, A., and Legendre, J. Y. (2001) Determination of the aqueous solubility of drugs using a convenient 96-well plate-based assay. *Drug Dev. Ind. Pharm.* 27 (1), 107−109.

(34) Trapella, C., Pela, M., Del Zoppo, L., Calo, G., Camarda, V., Ruzza, C., Cavazzini, A., Costa, V., Bertolasi, V., Reinscheid, R. K., Salvadori, S., and Guerrini, R. (2011) Synthesis and separation of the enantiomers of the neuropeptide S receptor antagonist (9R/S)-3-oxo-1,1-diphenyl-tetrahydro-oxazolo[3,4-a]pyrazine-7-carboxylic acid 4-fluoro-benzylamide (SHA 68). *J. Med. Chem.* 54 (8), 2738−2744.

(35) Flack, H. D. (1983) On Enantiomorph-Polarity Estimation. *Acta Crystallogr.* A39, 876−881.